GPC3 in terms of IGF2-induced cell proliferation, FGF2-induced cell proliferation was markedly suppressed by overexpressed GPC3 in HY-Toff cells. As for the inhibitory growth factors, BMP-7 suppressed the growth rate of HY-Toff cells in the absence of GPC3 expression, whereas the activity of BMP-7 was significantly blocked under conditions of an overexpression of GPC3. On the other hand, TGF-β had no effect on the cell proliferation of HY-Toff cells in the presence or absence of GPC3 overexpression. Overexpression of GPC3 also could not block the actions of HB-EGF.

GPC3 binds FGF2 in vivo

It has been previously demonstrated that GPC3 binds to FGF2 *in vitro*.[12] To confirm that GPC3 binds to FGF2 *in vivo*, FGF2 was cotransfected in HY-Toff-GPC3 cells and the interaction of GPC3 with FGF2 was investigated by immunoprecipitation assay. First, whole lysate was immunoprecipitated with an anti-GPC3 antibody bound to protein G beads, and the immunoprecipitates were analyzed by Western blot analysis with anti-FGF2 antibody. As shown in Figure 7*a*, FGF2 bound to GPC3 was detected. In the same manner, GPC3 interacting with FGF2 was confirmed by immunoprecipitation of FGF2, followed by Western blotting of GPC3 (Fig. 6*b*). The binding of GPC3 and FGF2 was thus demonstrated *in vivo*.

Enhanced expression of GPC3 inhibits the BMP-7 signaling pathway

To examine the effects of GPC3 on the BMP-7 signaling pathway, we compared the effects of the luciferase activity induced by BMP-7 in the presence or absence of enhanced expression of GPC3. In this model, ligand-induced functional activation is monitored by means of a luciferase reporter gene linked in its promoter region to a BMP-responsive element of Smad6. BMP-7-induced transcriptional activation of 3GC2-Lux was suppressed by the overexpression of GPC3. With high doses of BMP-7, the increase of luciferase activity was about 2.5-fold, in the absence of expres-

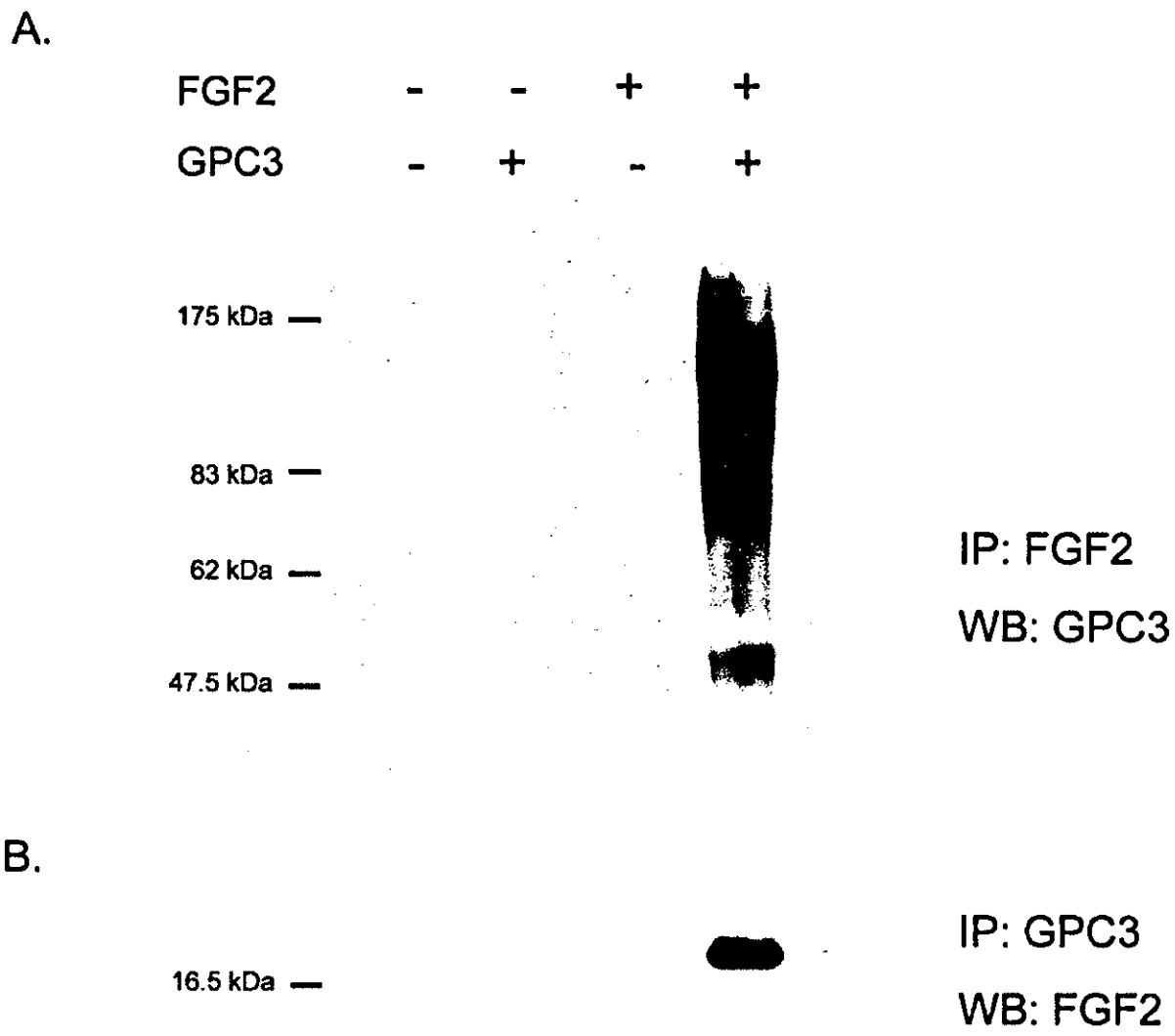

FIGURE 6 – Binding of GPC3 and FGF2 protein in HY-Toff cells. FGF2 was transiently transfected in HY-Toff-GPC3 cells and the expression of GPC3 was controlled by administration of Dox. The complex of FGF2 and GPC3 was co-immunoprecipitated by the anti-FGF2 *(a)* or anti-GPC3 *(b)* antibody. The coreprotein of GPC3 is truncated in the vicinity of N-terminus and the smaller size of coreprotein instead of the expected 65 kD is detected in this experiment (Oizumi *et al.*, unpublished data). IP, immunoprecipitation; WB, Western blotting.

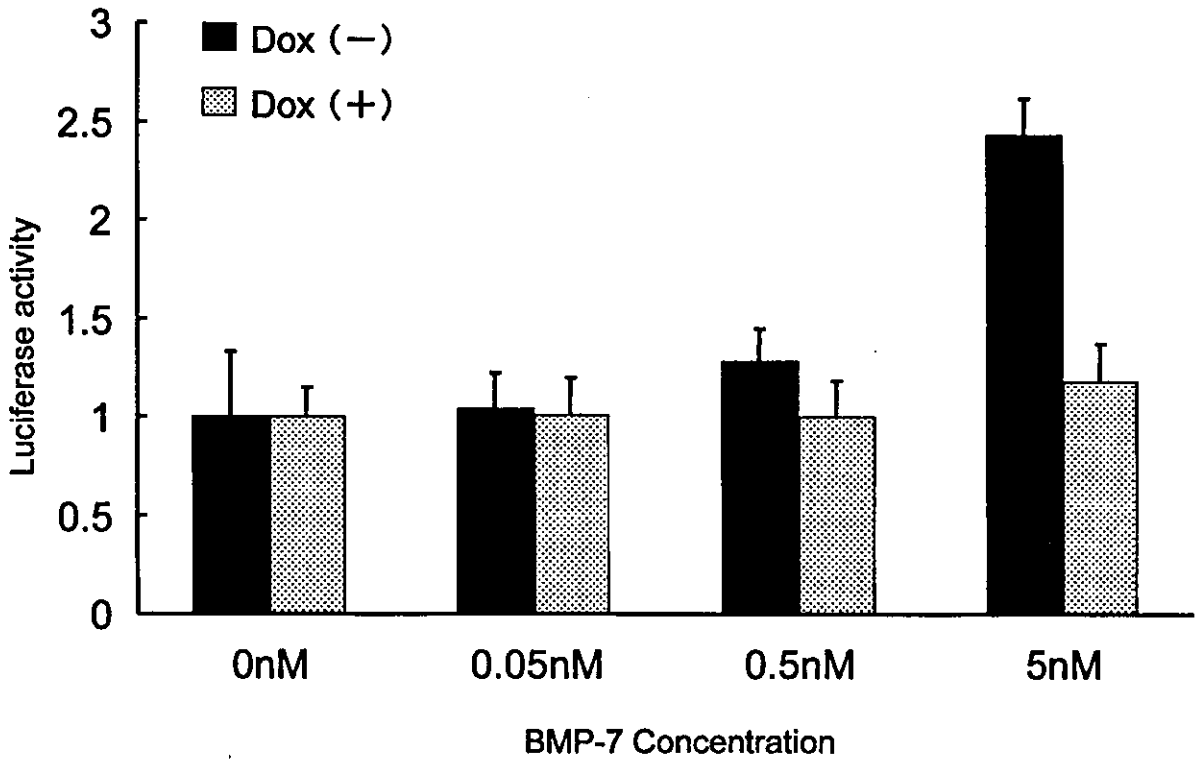

FIGURE 7 – Effects of enhanced GPC3 expression on BMP-7 signaling in HY-Toff cells. A fragment of the mouse Smad6 gene promoter, including the BMP-responsive element, was inserted into pGL2-Basic, and transcriptional activation activity was determined by luciferase assay in the presence (black bars) or absence (dotted bars) of Doxycycline using HY-Toff cells. Results are shown as fold-induction compared to the control cultures in the absence of BMP-7. Error bars represent standard deviations.

sion of GPC3. In contrast, overexpressed GPC3 strongly suppressed luciferase activity, even at the highest dose of BMP-7 (Fig. 7).

DISCUSSION

Recently, the overexpression of the mRNA for GPC3 has been demonstrated in embryonal tumors,[16] colon cancer[17] and HCC.[18,19] Our data based on oligonucleotide array analysis shows that GPC3 mRNA is highly expressed in 72% of liver cancer tissues even in 50% of WD. Moreover, the positive rate of GPC3 mRNA is higher than that of AFP, a tumor marker for HCC. This fact suggests that GPC3 is overexpressed in the early stage of HCC progression and may play a pivotal role in hepatocarcinogenesis. We also investigated expression of other members of glypican families using oligonucleotide array data, because glypican 1 has been reported to be upregulated in various cancers, such as pancreatic cancer and breast cancer.[26,27] U95A chip of GeneChip contains Glypican 1, 3, 4 and 5, and our data shows that glypican members except GPC3 were not upregulated in HCC compared to noncancerous tissues.

It has not been demonstrated that the GPC3 protein is in fact overexpressed in these cancers and this cancer-related cell line. Accordingly, to confirm overexpression of the GPC3 protein in HCC, we generated an anti-GPC3 monoclonal antibody and demonstrated it by Western blot and immunohistochemical analysis using hepatoma cell lines and surgically resected specimens. Although there was a slight discrepancy between the positive rate in HCC on Western blot and Northern blot analysis, the intensity of the expression of the GPC3 mRNA and 65 kDa protein in the resected specimens were significantly correlated. In the hepatoma cell lines HepG2, Hep3B, HT17, HuH6, HuH7 and PLC/PRF/5, which exhibited moderate to high levels of GPC3 mRNA, they also exhibited a high expression of GPC3 in translation. In contrast, HLE and Li7, in which the GPC3 mRNA was not demonstrated, there was no signal of the GPC3 protein via Western blot analysis. Immunohistochemical analysis revealed a clear pattern of immunoactivity at the cell surface of HCC and, therefore, led us to believe that GPC3 protein is also overexpressed in HCC.

However, an upregulation of GPC3 in cancerous tissues would be contradictory to the function of this molecule as it is generally understood, and therefore, we endeavored to elucidate how an upregulation of GPC3 could exert a positive effect on cancer cell growth. We first observed whether an overexpression of GPC3 in HY-Toff cells is able to accelerate their progression. However, the cell proliferation rate was not altered by the presence or absence of GPC3 expression. We then directed attention to studying the effects of GPC3 on the heparin-binding growth factors, IGF2 and FGF2, as well as on the TGF-β superfamily, BMP-7 and TGF-β3 because the HSPGs have been shown to interact with the heparin-binding growth factors and have been implicated in the signaling mediated by the TGF-β families.[1,2,28]

It is controversial whether GPC3 can exert control over the activity of IGF2. Pilia *et al.* reported that GPC3 forms a complex with IGF2 and negatively regulates IGF2 activity by competing for IGF2 binding with the signaling receptor.[11] At the same time, IGF2R, which is known to be a negative regulator of IGF2, in IGF2-deficient mice does not exhibit any in its levels.[29] In addition, no direct interaction between IGF2 and GPC3 to date has been reported.[12] And our data from a cell growth assay did show that an enhanced expression of GPC3 was not able to alter cell proliferation induced by IGF2.

HSPGs are known to be coreceptors for FGF2, strongly promoting FGF-FGFR binding and the subsequent activation of the receptor.[30,31] For example, syndecan-2 promotes FGF2-mediated proliferation,[32] and glypican-1 stimulates the FGF2 signaling pathway.[26] On the other hand, it has also been reported that endothelial proteoglycans inhibit FGF2 binding and mitogenesis.[6] Mali *et al.* demonstrated that an overexpression of syndecan-1 inhibits FGF2-induced growth promotion and at the same time does not control the binding of FGF2 at the cell surface.[5] Consistent with these data, our findings show that an enhanced expression of GPC3 in HY-Toff cells inhibits the stimulatory effect of FGF2 on cell proliferation through the interaction between GPC3 and FGF2, which is compatible with the function of GPC3.

Like FGF2, HB-EGF is known to have strong affinity for heparin,[33] and the growth rate of HY-Toff cells was accelerated by HB-EGF in cell growth assay. In our study, induced expression of GPC3 did not affect cell proliferation, which suggests that HB-EGF signaling is independent of GPC3.

In contrast, the overexpression of GPC3 was also shown to exert control over the inhibitory growth factor, BMP-7. BMP-7 is known to control tubule cell proliferation and apoptosis in a dose-dependent manner via Smad1-dependent and -independent pathways,[10] and GPC3 has been demonstrated to modulate the effects of BMP-7 in the kidney of the GPC3-/mouse.[4,34] Our data depict similar effects of GPC3 on BMP-7 in liver cancer, that is, BMP-7 controls the cell proliferation of hepatoma cell lines and an enhanced expression of GPC3 is able to exert control over the BMP-7-induced inhibitory effects in hepatoma cell proliferation. Moreover, by means of reporter gene assay with the Smad6 promoter, which contains a BMP-responsive element, we showed that overexpression of GPC3 actually inhibits the transcriptional activation induced by BMP-7. This function of GPC3 exerting control over the effect of an inhibitory growth factor is consistent with the extent of the upregulation of this molecule in HCC in our data.

In our study, we have demonstrated an overexpression of GPC3 in HCC. This molecule has been identified as a suppression of cell proliferation, and therefore, the fact that GPC3 interacts with FGF2 by inhibiting the activity of this growth factor is not surprising. At the same time, GPC3 also acts as a negative regulator of the inhibitory growth factor, BMP-7, controlling its transcriptional activation. Thus, GPC3 is able to not only inhibit cell proliferation in certain contexts but also can promote carcinogenesis in liver and other forms of cancer in others. To elucidate precisely, such different actions in these differing contexts will be important to understand the role GPC3 plays in the promotion of or protection against carcinogenesis in different biologic milieu. In addition, the ability of HCC cells to express GPC3 at high levels hints that GPC3 is possibly secreted in the serum of HCC patients and may serve as a new tumor marker for HCC.

ACKNOWLEDGEMENTS

We thank Dr. S. Tsutsumi for assistance with statistical analysis, Dr. H. Taniguchi for assistance with immunostaining, Dr. Y. Hippo for helpful discussion and Mrs. E. Ashihara, Miss S. Fukui and Miss H. Meguro for valuable technical assistance. We also thank Dr. K. Boru of Advanced Clinical Trials, Inc., for review of the manuscript.

REFERENCES

1. Filmus J, Selleck SB. Glypicans: proteoglycans with a surprise. J Clin Invest 2001;108:497–501.
2. Zhang Z, Coomans C, David G. Membrane heparan sulfate proteoglycan-supported FGF2-FGFR1 signaling. Evidence in support of the "cooperative end structures" model. J Biol Chem 2001;276:41921–9.
3. Paine-Saunders S, Viviano BL, Zupicich J, Skarnes WC, Saunders S. Glypican-3 controls cellular responses to Bmp4 in limb patterning and skeletal development. Dev Biol 2000;225:179–87.
4. Grisaru S, Cano-Gauci, Tee J, Filmus J, Rosenblum ND. Glypican-3 modulates BMP- and FGF-mediated effects during renal branching morphogenesis. Dev Biol 2001;231:31–46.
5. Mali M, Elenius K, Miettinen HM, Jalkanen M. Inhibition of basic fibroblast growth factor-induced growth promotion by overexpression of syndecan-1. J Biol Chem 1993;268:24215–22.
6. Forsten KE, Courant NA, Nugent MA. Endothelial proteoglycans inhibit bFGF binding and mitogenesis. J Cell Physiol 1997;172:209–20.
7. Filla MS, Dam P, Rapraeger AC. The cell surface proteoglycan syndecan-1 mediates fibroblast growth factor-2 binding and activity. J Cell Physiol 1998;174:310–21.
8. Clasper S, Vekemans S, Fiore M, Plebanski M, Wordsworth P, David G, Jackson DG. Inducible expression of the cell surface heparan sulfate proteoglycan syndecan-2 (fibroglycan) on human activated macrophages can regulate fibroblast growth factor action. J Biol Chem 1999;274:24113–23.
9. Clayton A, Thomas J, Thomas GJ, Davies M, Steadman R. Cell surface heparan sulfate proteoglycans control the response of renal interstitial fibroblasts to fibroblast growth factor-2. Kidney Int 2001; 59:2084–94.
10. Piscione TD, Phan T, Rosenblum ND. BMP7 controls collecting tubule cell proliferation and apoptosis via Smad1-dependent and -independent pathways. Am J Physiol Renal Physiol 2001;280:F19–33.
11. Pilia G, Hughes-Benzie RM, MacKenzie A, Baybayan P, Chen EY, Huber R, Neri G, Cao A, Forabosco A, Schlessinger D. Mutations in GPC3, a glypican gene, cause the Simpson-Golabi-Behmel overgrowth syndrome. Nat Genet 1996;12:241–7.
12. Song HH, Shi W, Filmus J. OCI-5/rat glypican-3 binds to fibroblast growth factor-2 but not to insulin-like growth factor-2. J Biol Chem 1997;272:7574–7.
13. Gonzalez AD, Kaya M, Shi W, Song H, Testa JR, Penn LZ, Filmus J. OCI-5/GPC3, a glypican encoded by a gene that is mutated in the Simpson-Golabi-Behmel overgrowth syndrome, induces apoptosis in a cell line-specific manner. J Cell Biol 1998;141:1407–14.
14. Lin H, Huber R, Schlessinger D, Morin PJ. Frequent silencing of the GPC3 gene in ovarian cancer cell lines. Cancer Res 1999;59:807–10.
15. Murthy SS, Shen T, De Rienzo A, Lee WC, Ferriola PC, Jhanwar SC, Mossman BT, Filmus J, Testa JR. Expression of GPC3, an X-linked recessive overgrowth gene, is silenced in malignant mesothelioma. Oncogene 2000;19:410–6.
16. Saikali Z, Sinnett D. Expression of glypican 3 (GPC3) in embryonal tumors. Int J Cancer 2000;89:418–22.
17. Lage H, Dietel M, Froschle G, Reymann A. Expression of the novel mitoxantrone resistance associated gene MXR7 in colorectal malignancies. Int J Clin Pharmacol Ther 1998;36:58–60.
18. Hsu HC, Cheng W, Lai PL. Cloning and expression of a developmentally regulated transcript MXR7 in hepatocellular carcinoma: biological significance and temporospatial distribution. Cancer Res 1997;57:5179–84.
19. Zhu ZW, Friess H, Wang L, Abou-Shady M, Zimmermann A, Lander AD, Korc M, Kleeff J, Buchler MW. Enhanced glypican-3 expression differentiates the majority of hepatocellular carcinomas from benign hepatic disorders. Gut 2001;48:558–64.
20. Tsuda H, Oda T, Sakamoto M, Hirohashi S. Different pattern of chromosomal allele loss in multiple hepatocellular carcinomas as evidence of their multifocal origin. Cancer Res 1992;52:1504–9.
21. Huang Y, Uchiyama Y, Fujimura T, Kanamori H, Doi T, Takamizawa A, Hamakubo T, Kodama T. A human hepatoma cell line expressing hepatitis c virus nonstructural proteins tightly regulated by tetracycline. Biochem Biophys Res Commun 2001;281:732–40.
22. Hippo Y, Yashiro M, Ishii M, Taniguchi H, Tsutsumi S, Hirakawa K, Kodama T, Aburatani H. Differential gene expression profiles of scirrhus gastric cancer cells with high metastatic potential to peritoneum or lymph nodes. Cancer Res 2001;61:889–95.
23. Kohler G, Milstein C. Continuous cultures of fused cells secreting antibody of predefined specificity. Nature 1975;256:495–7.
24. Matsuda K, Maruyama H, Guo F, Kleeff J, Itakura J, Matsumoto Y, Lander AD, Korc M. Glypican-1 is overexpressed in human breast cancer and modulates the mitogenic effects of multiple heparin-binding growth factors in breast cancer cells. Cancer Res 2001;61: 5562–9.
25. Ishida W, Hamamoto T, Kusanagi K, Yagi K, Kawabata M, Takehara K, Sampath TK, Kato M, Miyazono K. Smad6 is a Smad1/5-induced smad inhibitor. Characterization of bone morphogenetic protein-responsive element in the mouse Smad6 promoter. J Biol Chem 2000; 275:6075–9.
26. Kleeff J, Ishiwata T, Kumbasar A, Friess H, Buchler MW, Lander AD, Korc M. The cell-surface heparan sulfate proteoglycan glypican-1 regulates growth factor action in pancreatic carcinoma cells and

is overexpressed in human pancreatic cancer. J Clin Invest 1998;102: 1662–73.
27. Matsuda K, Maruyama H, Guo F, Kleeff J, Itakura J, Matsumoto Y, Lander AD, Korc M. Glypican-1 is overexpressed in human breast cancer and modulates the mitogenic effects of multiple heparin-binding growth factors in breast cancer cells. Cancer Res 2001;61: 5562–9.
28. Blackhall FH, Merry CL, Davies EJ, Jayson GC. Heparan sulfate proteoglycans and cancer. Br J Cancer 2001;85:1094–8.
29. Ludwig T, Eggenschwiler J, Fisher P, D'Ercole AJ, Davenport ML, Efstratiadis A. Mouse mutants lacking the type 2 IGF receptor (IGF2R) are rescued from perinatal lethality in Igf2 and Igf1r null backgrounds. Dev Biol 1996;177:517–35.
30. Yayon A, Klagsbrun M, Esko JD, Leder P, Ornitz DM. Cell surface, heparin-like molecules are required for binding of basic fibroblast growth factor to its high affinity receptor. Cell 1991;64:841–8.
31. Steinfeld R, Van Den Berghe H, David G. Stimulation of fibroblast growth factor receptor-1 occupancy and signaling by cell surface-associated syndecans and glypican. J Cell Biol 1996;133:405–16.
32. Clasper S, Vekemans S, Fiore M, Plebanski M, Wordsworth P, David G, Jackson DG. Inducible expression of the cell surface heparan sulfate proteoglycan syndecan-2 (fibroglycan) on human activated macrophages can regulate fibroblast growth factor action. J Biol Chem 1999;274:24113–23.
33. Thompson SA, Higashiyama S, Wood K, Pollitt NS, Damm D, McEnroe G, Garrick B, Ashton N, Lau K, Hancock N, Klagsbrun N, Abraham JA. Characterization of sequences within heparin-binding EGF-like growth factor that mediate interaction with heparin. J Biol Chem 1994;269: 2541–9.
34. Cano-Gauci DF, Song HH, Yang H, McKerlie C, Choo B, Shi W, Pullano R, Piscione TD, Grisaru S, Soon S, Sedlackova L, Tanswell AK, et al. Glypican-3-deficient mice exhibit developmental overgrowth and some of the abnormalities typical of Simpson-Golabi-Behmel syndrome. J Cell Biol 1999;146:255–64.

ELSEVIER

Journal of Hepatology 37 (2002) 31–38

Journal of Hepatology

www.elsevier.com/locate/jhep

Effects of amrinone on hepatic ischemia–reperfusion injury in rats☆

Takashi Kobayashi, Yasuhiko Sugawara*, Takao Ohkubo, Hiroshi Imamura, Masatoshi Makuuchi

Hepato-Biliary-Pancreatic Division, Department of Surgery, Graduate School of Medicine, University of Tokyo, 7-3-1 Hongo, Bunkyo-ku, Tokyo 113-8655, Japan

***Background/Aims*: The present study was designed to investigate the effect of amrinone, a phosphodiesterase III inhibitor, on hepatic ischemia–reperfusion injury in rats.**

***Methods*: Amrinone was infused at a rate of 20 or 100 μg/kg/min, and 60-min partial ischemia was induced. The effects of amrinone on hemodynamic status, hepatic tissue cyclic adenosine 5′-monophosphate (cAMP), hepatic tissue blood flow, platelet aggregation and plasma levels of transaminase were examined. The expression of intercellular adhesion molecule-1 (ICAM-1) and myeloperoxidase activity were analyzed and histological examination was performed in the injured liver. The cumulative survival rates for 14 days were also examined.**

***Results*: Hemodynamic status was not affected by amrinone. The levels of cAMP during reperfusion were significantly higher in rats with amrinone. Hepatic tissue blood flow during reperfusion was increased and platelet aggregation was inhibited by amrinone. The expression of ICAM-1 mRNA and protein in the injured liver was suppressed in rats with amrinone. The levels of transaminase, necrotic changes and myeloperoxidase activity were suppressed after reperfusion and higher survival was achieved in the rats treated with amrinone.**

***Conclusions*: Amrinone protected against ischemia–reperfusion injury of the liver in the present model.**

***Keywords*: Hepatic tissue blood flow; Liver ischemia/reperfusion injury; Platelet aggregation; Phosphodiesterase III inhibitor**

1. Introduction

Amrinone (Amcoral, Meiji Pharmaceutical Co. Ltd., Tokyo, Japan) is a non-catecholamine, non-glycoside drug with combined positive inotropic and vasodilating properties. Its mechanism of action is mediated by selective phosphodiesterase III enzyme inhibition, which increases cyclic adenosine 5′-monophosphate (cAMP) in both vascular smooth muscle and myocardium by preventing the degradation of cAMP [1–3].

Increased cAMP increases muscle contractions by increasing myocardial intracellular calcium available from the sarcoplasmic reticulum. In contrast, in vascular smooth muscle cells, increased cAMP decreases intracellular calcium through an increase in calcium re-sequestration into the sarcoplasmic reticulum, producing relaxation and vasodilatation. Since amrinone not only augments cardiac contractility but also reduces preload and afterload, it has been used to treat heart failure [4,5]. It has been reported that amrinone inhibited agonist-induced calcium mobilization, platelet activation and the expression of adhesion molecules such as intercellular adhesion molecule-1 (ICAM-1).

The pharmacological action of amrinone appears to be ideal for treating peripheral circulatory disorders and improving the viability of ischemic tissues. We hypothesized that amrinone could also be useful for treating ischemic liver. This study was designed to evaluate the effects of amrinone on the liver damaged by ischemia/reperfusion injury.

2. Materials and methods

2.1. Animals

Male Wistar rats weighing between 300 and 350 g were purchased from

Received 20 June 2001; received in revised form 25 February 2002; accepted 1 March 2002

☆ The authors of this study state that they have no relationship past or present with the pharmaceutical company involved with the drugs mentioned in the study, neither have they received funding from the companies.

* Corresponding author. Tel.: +81-3-3815-5411; fax: +81-3-5684-3989.
E-mail address: yasusuga-tky@umin.ac.jp (Y. Sugawara).

0168-8278/02/$20.00
PII: S0168-8278(02)00084-3

Nippon Bio-Supplement Center, Tokyo. Japan. They were fed a commercial pelleted diet and water ad libitum in a cage at 22 ± 2 °C under normal lighting conditions. After overnight fasting, they were anesthetized with an intra-peritoneal injection of 50 mg/kg body weight of pentobarbital sodium, and placed supine on a heating pad (36–37 °C). The following protocols were approved by the Animal Research Committee of the University of Tokyo.

The left extra jugular vein was cannulated with a polyethylene catheter (PE-90, Natsume Seisakusho Ltd., Tokyo, Japan). In a control (C) group, physiological saline (8 ml/kg per h, group) was infused continuously. In the amrinone-treated groups, after a dose of 1 mg/kg body weight was injected through a penile vein, amrinone was continuously infused at a dose of 20 or 100 μg/kg per min (8 ml/kg per h, 20G and 100G groups, respectively).

The total number of the rats used for the study was 241, consisting of 15 for hemodynamic measurement, 15 for measurement of hepatic tissue blood flow, 75 for blood sampling, 91 for liver tissue sampling and 45 for survival analysis.

2.2. Measurement of the effects of amrinone on hemodynamic changes

A polyethylene catheter (PE-50, Natsume Seisakusho Ltd.) was inserted into the right carotid artery to measure mean arterial blood pressure (MABP) and heart rate (HR). The catheter was connected to a blood pressure transducer (Gould Statham P23 1D, Hatorey, PR). The trachea was cannulated and connected to a small animal ventilator (Ugo Basil 7025, Milan, Italy). The rats were ventilated with room air. After a midsternal thoracotomy was performed, an electromagnetic flow probe (Skalar MDL1401, Amsterdam, Holland) was placed around the ascending aorta to measure cardiac output (CO).

After these surgical maneuvers, the infusion of physiological saline or amrinone was started and continued for 3 h. Fifteen animals were used ($n = 5$ for each group). The parameters were recorded as a percentage of the initial value. Measurements were scheduled at 0, 15, and 30 min, and at 1, 2 and 3 h after beginning infusion.

2.3. Ischemia induction and measurement of hepatic tissue blood flow

After laparotomy was made in a midline incision, the left branches of both the portal vein and hepatic artery were clamped with a microvascular clip for 60 min to establish liver ischemia while preventing portal congestion. The clip was then released to induce reperfusion. To compensate for evaporative losses during the surgical preparation, infusion was started 30 min before the induction of hepatic ischemia, which was continued 3 h after reperfusion. The total infusion duration was 270 min in the present study and experiments for blood or liver sampling.

Hepatic tissue blood flow was measured using a laser-Doppler flow meter (ALF 2100, Advance Co., Tokyo, Japan) 30 min before the induction of ischemia, and 0, 1, 2 and 3 h after reperfusion, as described previously [6]. Each value was recorded as a percentage of the pre-ischemic value. Fifteen animals were used ($n = 5$ for each group).

2.4. Blood samples and assays

Blood samples were collected from the abdominal aorta to measure aspartate aminotransferase (AST) and alanine aminotransferase (ALT) before ischemic insult, and 0, 2 and 5 h after reperfusion ($n = 5$ for each group and each time point). Blood samples were centrifuged at 4 °C for 15 min at $1200 \times g$ in glass tubes, and the plasma was stored at −80 °C in polystyrene tubes until use, as described previously [7].

Platelet aggregation was measured as described previously [8]. Briefly, blood samples taken 90 min after reperfusion were collected in a syringe containing 1:9 sodium citrate. Platelet-rich plasma was obtained by centrifugation at 4 °C for 10 min at $150 \times g$. Platelet aggregation was induced by adenosine diphosphate (final concentration, 100 μmol/l). Light transmission for adenosine diphosphate was recorded for 10 min after a 2-min incubation period. The maximal aggregation response was taken as the area under the aggregation curves. Fifteen animals were used for the measurement ($n = 5$ for each group).

2.5. Liver sampling and assays

Parts of the left lateral lobes of the liver were taken to measure cAMP and the expression of ICAM-1, and for a histological examination.

For cAMP measurement, the liver specimens just before ischemia and reperfusion, and 0, 15 and 60 min after reperfusion ($n = 5$/group/time point) were used. Liver tissue cAMP was determined as described previously [9]. Briefly, the specimen was immersed in liquid nitrogen, which was then homogenized in ice-cold 6% trichloroacetic-acid solution and centrifuged. The extraction was performed twice. The supernatant was analyzed for cAMP using an RIA kit (Cyclic AMP Lit, Yamasa Co., Chiba, Japan).

To examine the expression of ICAM-1, liver specimens taken 3 (for mRNA analysis and myeloperoxidase assay) and 6 h (for immunohistochemistry analysis, Western blotting, myeloperoxidase assay, histological analysis and assay for apoptotic cells) after reperfusion. Five rats in each group were used. One sham operated rat was used as a negative control.

2.6. Reverse transcription-polymerase chain reaction

The expression of ICAM-1 and β-actin was analyzed by reverse transcription-polymerase chain reaction (RT-PCR). Total RNA was isolated [10] and 5 μg RNA was used for complementary DNA synthesis. PCR was performed at the following temperatures: for ICAM-1, denaturation at 94 °C for 45 s, primary annealing at 55 °C for 30 s and primer extension 72 °C for 90 s [11,12]; and for β-actin, 94 °C for 1 min, 55 °C for 1 min and 72 °C for 2 min [13]. The sequences of the primer sets were GAT GCT GAC CCT GGA GAG CA and CAG GGA CTT CCC ATC CAC CT for ICAM-1 [13]. Those for β-actin were TAT GGA ATC CTG TGG CAT CC and ACA GAA GCA ATG CTG TCA CC [11]. The corrected fluorescence activity of ICAM-1 was evaluated as described previously [7].

2.7. Immunohistochemistry

Five-micrometer-thick sections were cut from every specimen taken 6 h after reperfusion, fixed in neutral formalin and processed for routine histology, as described previously [14]. The sections were incubated overnight with monoclonal antibodies against rat ICAM-1 (Seikagaku Corporation, Tokyo, Japan) at a concentration of 5 μg/ml.

2.8. Western blotting

The details for the analysis have been described elsewhere [15]. In brief, protein was extracted from liver tissue and 5 μg was used for analysis. Its concentration was assayed by a modification of Lowry's method [16]. The sample was electrophoresed in 10% polyacrylamide gel, and then transferred to a nitrocellulose membrane. The expression of ICAM-1 was confirmed using monoclonal antibodies against rat ICAM-1 (Seikagaku Corporation) at a concentration of 5 μg/ml.

2.9. Myeloperoxidase assay

The details for the assay have been described elsewhere [17]. In brief, liver specimens taken 3 or 6 h after reperfusion were thawed at room temperature, weighed and homogenized in ice-cold potassium phosphate buffer (20 mM, pH 7.4). A 25 μl tissue sample was diluted in 80 mM potassium phosphate buffer (pH 5.4). Then 150 μl of *o*-dianidine and hydrogen peroxide diluted in potassium phosphate buffer (pH 5.4) were added to the sample. The mixture was incubated for 5 min at 37 °C in 96 well microtiter plates with 3,3′,3,5′-tetramethylbenzidine (Sigma Chemical Co, St. Louis, MO). One unit of myeloperoxidase activity was defined as the amount of enzyme reducing 1 μmol peroxide/min.

2.10. Histological examination

Liver specimens collected after 6 h of reperfusion were stored in 10% (w/w) formaldehyde solution, embedded in paraffin and stained with hematoxylin and eosin. The degree of liver necrosis was evaluated semiquantitatively according to previous guidelines [18]: none, 0; individual-cell necrosis, 1; up to 30% lobular necrosis, 2; up to 60% lobular necrosis, 3; more than 60% lobular necrosis, 4. Slides were examined by a single histologist who was blind to the treatment groups.

2.11. Terminal deoxyribonucleotidyl-transferase-mediated dUTP-digoxigenin nick-end labeling assay

The tissue sections taken 6 h after reperfusion were used for the assay. DNA fragmentation was detected by performing a terminal deoxyribonucleotidyl-transferase-mediated dUTP-digoxigenin nick-end labeling (TUNEL) assay as indicated in the manufacturer's instructions (ApoTag Peroxidase In Situ Apoptosis Detection Kit, Intergen Co., Purchase, NY). The apoptotic cells were defined as the stained cells with cell shrinkage, nuclear condensation and apoptotic bodies. The numbers of the cells were counted in 20 high power (×400) fields and recorded as the ratio to total hepatocytes.

2.12. Survival

The cumulative survival rates for the first 14 days after ischemia/reperfusion injury were examined ($n = 15$ for each group).

2.13. Statistical analysis

Data are expressed as the means ± SEM. The statistical software package Stat View (SAS Institute, Inc., Cary, NC), version 5.0 for Windows, was used throughout the analysis. The levels of MABP, HR, and CO for each group were compared with the corresponding levels before the infusion of normal saline or amrinone. The levels of hepatic tissue blood flow, AST, ALT and cAMP were compared with the corresponding pre-ischemia levels in each group. Differences were evaluated by an analysis of variance (ANOVA) with Bonferroni's correction.

The biological effect of amrinone on the level of each factor during the observation period was evaluated among the groups by ANOVA (platelet aggregation, ICAM-1 mRNA level, myeloperoxidase activity, TUNEL assay and the degree of necrosis) or two-way repeated-measures ANOVA (the other factors).

Survival rates were calculated by the Kaplan–Meier method and those among the groups were compared using the log-rank test.

The results were considered significant at $P < 0.008$ or $P < 0.005$ for ANOVAs and at $P < 0.05$ for the other analyses.

3. Results

3.1. Effects of amrinone on hemodynamics (Fig. 1)

MABP, HR and CO remained unchanged throughout the observation period in all groups. There was no significant difference in these parameters among the groups.

3.2. Effects of amrinone on liver tissue cAMP (Fig. 2)

There was a notable decline in tissue cAMP during the initial 15 min of reperfusion in the control group ($P < 0.001$), and this was not recovered at 60 min after the end of ischemia. In contrast, cAMP levels increased during reperfusion in the 20G and 100G groups. cAMP levels in the 20G and 100G groups differed significantly from the control during the observation period ($P = 0.03$ and $P = 0.01$ for each comparison).

3.3. Effects of amrinone on hepatic tissue blood flow (Fig. 3)

In all of the groups, hepatic tissue blood flow decreased significantly ($P < 0.001$) after the induction of ischemia, but then recovered to the pre-ischemic level at 2 h after

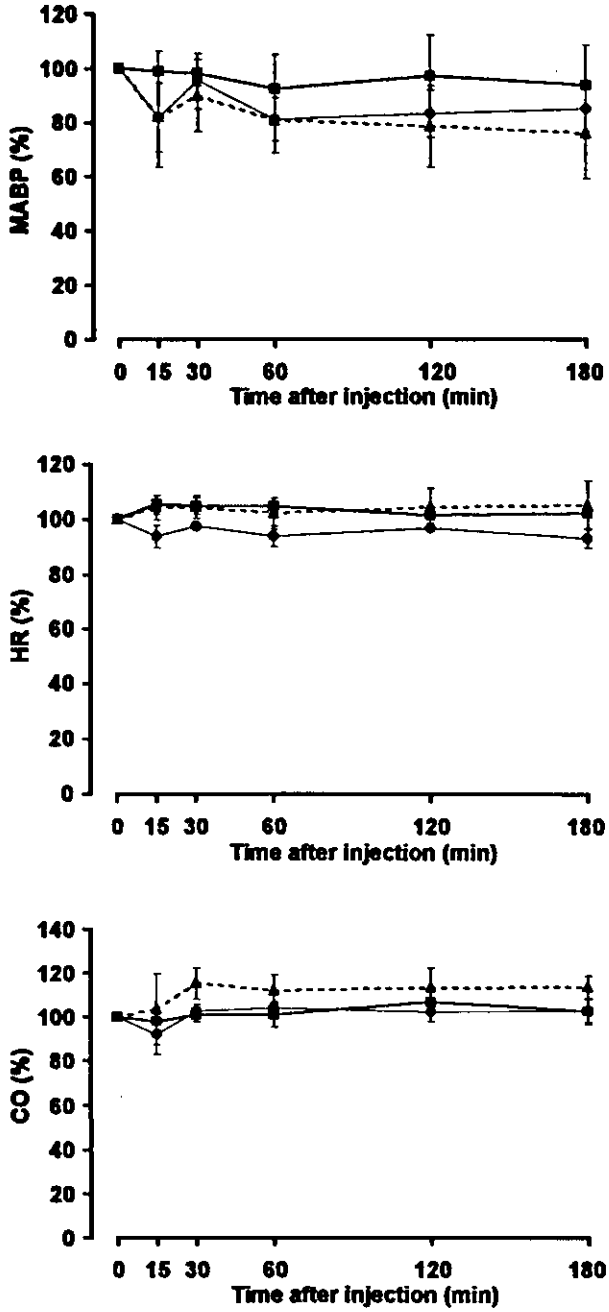

Fig. 1. MABP, HR and CO for 3 h after the infusion of physiological saline or amrinone. Values are expressed as a percentage of the initial level at 30 min before ischemia. Thin line, control group; thick line, amrinone (20 μg/kg per min)-treated group; broken line, amrinone (100 μg/kg per min)-treated group.

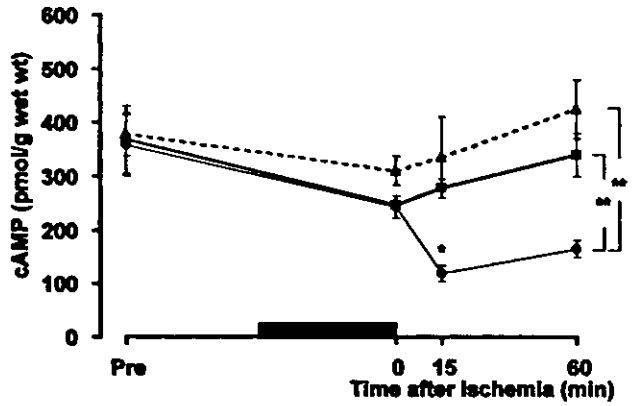

Fig. 2. Hepatic cAMP concentrations before ischemia, at reperfusion, and 15 and 60 min after reperfusion. *$P < 0.008$ compared with the average pre-ischemic level. Two-way repeated-measures ANOVA revealed that cAMP in the 20G or 100G group differed significantly from that in the control group ($P < 0.05$). The black box indicates the duration of ischemia.**

the induction of ischemia. Blood flow in 20G and 100G groups differed significantly from the control during the observation period ($P = 0.04$ and $P = 0.02$ for each comparison).

3.4. Effects of amrinone on platelet aggregation and ICAM-1 mRNA (Table 1, Fig. 4)

Platelet aggregation 90 min after reperfusion decreased in the amrinone-treated groups compared with that in the control ($P = 0.04$ for both comparison).

ICAM-1 mRNA expression was observed in ischemic liver tissues obtained 3 h after the induction of ischemia in all groups. Analysis of the densitometric data revealed

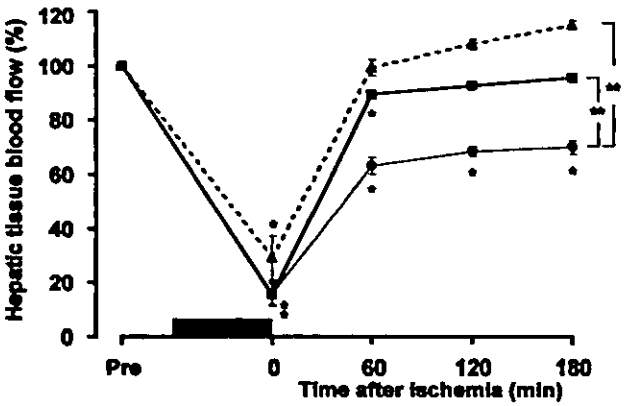

Fig. 3. Hepatic tissue blood flow in the liver before ischemia, just before reperfusion, and 1, 2, and 3 h after reperfusion. Values are expressed as a percentage of the initial level before ischemia. The black box indicates the duration of ischemia. *$P < 0.005$ compared with the average pre-ischemic level. Two-way repeated-measures ANOVA revealed that hepatic blood flow in the 20G or 100G group differed significantly from that in the control group ($P < 0.05$). The black box indicates the duration of ischemia.**

a significant difference among the groups with regard to the corrected fluorescence activity of ICAM-1.

3.5. Immunohistochemical analysis (Fig. 5)

ICAM-1 expression was detected mainly in hepatocyte cells around the central veins. Immunoreactivity was suppressed in the specimens in the 20G group.

3.6. Immunoblot analysis (Fig. 6)

Western blotting analysis revealed bands with an apparent molecular mass of 92 kDa (ICAM-1) in samples obtained from the liver in the control. No clear bands were detected in the specimens from the 20G and 100G groups.

3.7. Effects of amrinone on AST and ALT (Fig. 7)

In the 100G group, AST levels reached their maximum values 2 h after ischemic insult. In contrast, AST levels continued to increase during the observation period in the control and 20G groups. ALT levels showed changes similar to those of AST levels. Two-way repeated-measures ANOVA revealed that AST and ALT levels in the 20G and 100G groups differed significantly from those in the control group ($P = 0.01$ for each comparison).

3.8. Myeloperoxidase activity (Table 1)

The activity in the liver tissues obtained 6 h after reperfusion in 20G and 100G groups was significantly lower than that of the control ($P = 0.001$ and $P = 0.0005$ for each comparison).

3.9. Histological examination (Table 1)

In the control group, foci of necrosis with the infiltration of neutrophils were noted mainly in the hepatocytes around the central veins, and sinusoidal congestion and derangement were also apparent. In the amrinone groups, however, these changes were markedly suppressed. This result was confirmed by a semiquantitative assessment.

3.10. TUNEL assay (Table 1)

Approximately 0.4% of the hepatocytes were apoptotic in the control. The ratio was lower in the amrinone-treated rats. However, the difference was not statistically significant ($P = 0.24$ and $P = 0.12$ for each comparison).

3.11. Survival

The cumulative survival rates for the rats in the control, 20G and 100G groups for 14 days were 73.3 (11/15), 100 (15/15) and 100% (15/15), respectively. The rats in the 20G and 100G groups showed significantly better survival than those in the control ($P = 0.001$ for both comparison).

Table 1
Effect of amrinone on platelet aggregation, mRNA levels of adhesion molecules and histology

	Control ($n = 5$)	20G ($n = 5$)	100G ($n = 5$)
Platelet aggregation	6330 ± 449	3958 ± 531*	2843 ± 435*
ICAM-1 mRNA	2.4 ± 0.3	1.0 ± 0.1*	0.4 ± 0.05*
Myeloperoxidase (U/g)			
3 h after reperfusion	6.8 ± 2.4	1.9 ± 0.03*	2.8 ± 0.1
6 h after reperfusion	11.7 ± 1.7	2.9 ± 0.5*	1.8 ± 0.2*
Histology			
Necrotic changes (score)	1.9 ± 0.3	1.2 ± 0.2*	0.9 ± 0.2*
Apoptotic hepatocytes (%)	0.4 ± 0.05	0.3 ± 0.02	0.2 ± 0.03

* $P < 0.05$ compared with the control level.

4. Discussion

The present study provides new insight into the synergetic mechanism of amrinone toward the amelioration of hepatic warm ischemia–reperfusion injury. Amrinone suppressed the degradation of cAMP in injured liver tissues. Augmented hepatic tissue blood flow, inhibition of platelet aggregation and decreased expression of ICAM-1 mRNA and proteins were observed. The protective effects of amrinone were confirmed by the plasma transaminase levels, myeloperoxidase activity, histological findings and survival. Unexpectedly, the ratio of apoptotic cells did not differ between the control and amrinone-treated groups. The role for apoptosis in the lesions after ischemia–reperfusion injury seems to be controversial. Gujral and associates [19] revealed that only a small minority of rat hepatocytes underwent apoptosis after 60 min of warm ischemic insult. They concluded that the caspase inhibitors were not effective in attenuating the apoptotic changes of the hepatocytes. In contrast, a recent experiment [20] stressed the central role for apoptosis of endothelial cells and hepatocytes of rat liver after ischemia–reperfusion injury. Cursio and colleagues [21] suggested that caspase inhibitors had important therapeutic implications in liver ischemic diseases.

An excessive amount of amrinone might lead to severe hypotension, which would cause low perfusion in some organs due to its vasodilating effects. However, our results indicated that the amelioration of hepatic ischemia–reperfusion injury by amrinone was achieved independently of its inotropic effects on rat hemodynamics. Weishaar and associates [22] reported that imazodan-sensitive and -insensitive subclasses of cAMP-specific phosphodiesterase III existed in ventricular muscle in membrane-bound or soluble form. The membrane-bound form of the imazodan-sensitive subclass of phosphodiesterase III is important in modulating the inotropic response to imazodan and amrinone. However, the rat left ventricular muscle lacks this form of phosphodiesterase-III. This might explain why amrinone had a slight effect on rat CO in the present study.

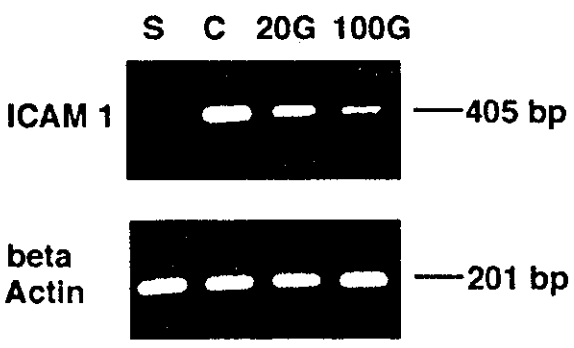

Fig. 4. Expression of ICAM-1 and β-actin in liver specimens taken 3 h after reperfusion by RT-PCR. S, sham operated rats; C, control group; 20G, 20G group; 100G, 100G group.

The present study showed that the decline in cAMP concentrations in the injured liver tissue after reperfusion was suppressed by the infusion of amrinone. cAMP has various physiologic effects that are beneficial to ischemia–reperfusion injury, including the preservation of transendothelial barrier function [23]. Pretreatment to increase intracellular cAMP has been shown to improve postischemic recovery in the liver [24]. At the cellular level, restoration of cAMP content was associated with a normalization of cell shape and barrier function for vascular endothelial cells [23,25].

A lack of microvascular flow due to vasoconstriction is an important factor in hepatic ischemia–reperfusion injury [26]. In the present study, a significant improvement in hepatic tissue blood flow was demonstrated in the injured tissues in amrinone-treated rats. The favorable results after ischemia/reperfusion injury in the amrinone-treated rats might be due to increased hepatic blood flow. Attention should be paid to the finding that hepatic arterial flow was increased although cardiac function was not improved significantly by amrinone infusion. One possible explanation is augmented hepatic blood flow through dilated hepatic vascular beds by hepatic arterial buffer response [27].

Platelet aggregation is a causative factor which aggravates ischemia–reperfusion injury [28]. The adherence of platelets to the hepatic vasculature after reperfusion had detrimental effects on the viability of human liver allografts [29]. Amrinone inhibited human platelet activation at the cellular level and protected against experimental coronary thrombosis in dogs [30]. In the present model, amrinone

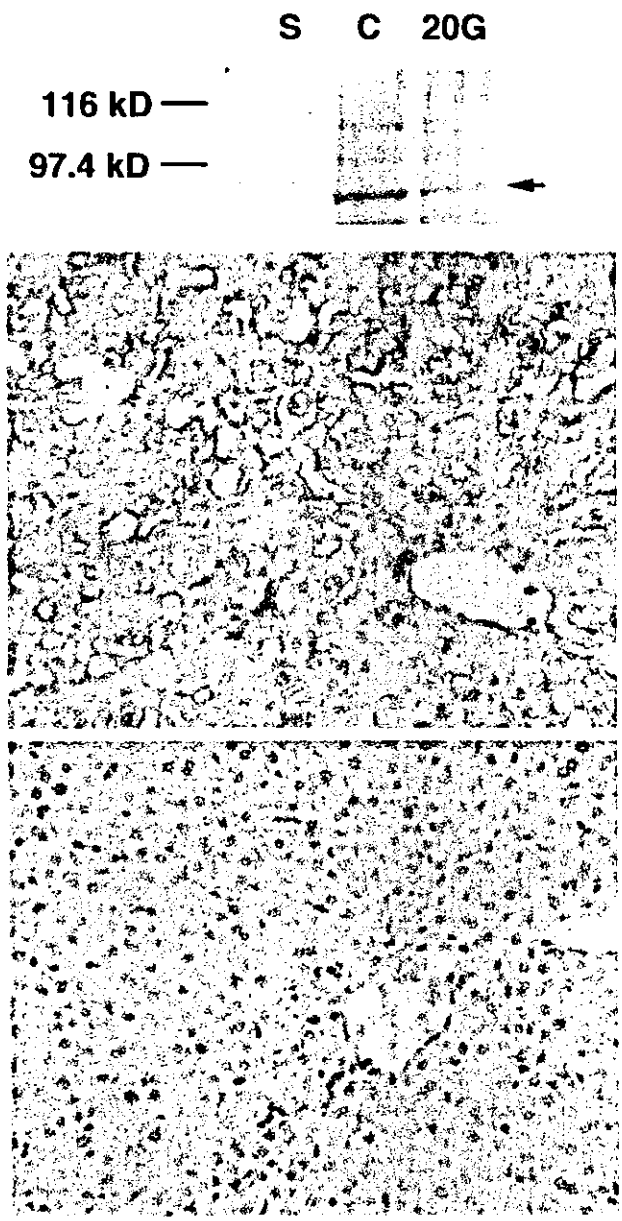

Fig. 5. Immunohistochemical staining for ICAM-1. ICAM-1 was expressed around hepatocytes around the central hepatic vein in the control group (A). Immunoreactivity was suppressed in the 20G group (B; original magnification, ×400).

significantly inhibited platelet aggregation, and this might be involved in the mechanism of the improvement of hepatic ischemia–reperfusion injury.

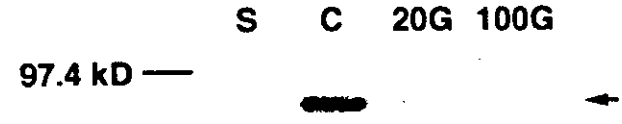

Fig. 6. ICAM-1 protein detection (arrow) by Western blotting. S, sham operated rats; C, control group; 20G, 20G group; 100G, 100G group.

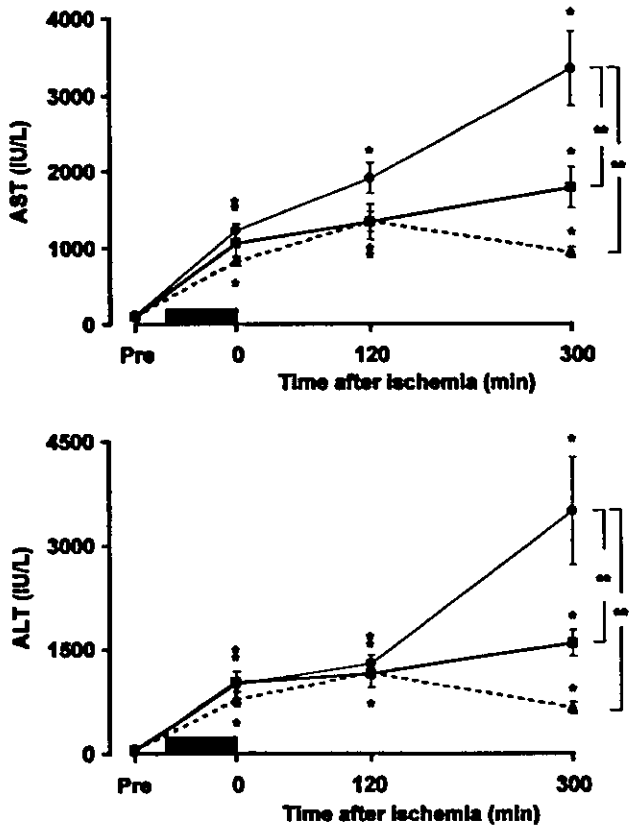

Fig. 7. Changes in AST and ALT levels. In the 100G group, AST and ALT levels reached their maximum values 2 h after ischemic insult. The levels of AST and ALT in the control group markedly increased during the observation period. *$P < 0.008$ compared with the average pre-ischemic level. Two-way repeated-measures ANOVA revealed that AST and ALT in the 20G or 100G group differed significantly from that in the control group (**$P < 0.05$). The black box indicates the duration of ischemia.

The adhesion of leukocytes to the microvascular endothelium is another cause of ischemia–reperfusion injury, and is mediated by a variety of cell-surface molecules [28]. ICAM-1 is one of these molecules, and is constitutively present at low levels on most endothelial cells [31] and is up-regulated by inflammation and ischemia–reperfusion injury [32]. Blocking the function of ICAM-1 adhesion receptors with monoclonal antibody has been shown to protect against liver ischemia–reperfusion injury [33,34]. The present study showed that amrinone regulates ICAM-1 expression at the gene-transcription stage and post-transcriptional protein modification, although the precise mechanism by which amrinone regulates ICAM-1 molecules was not elucidated in the present study.

In the previous report [35], 15 cirrhotic patients received amrinone infusion during hepatectomy for hepatocellular carcinoma. The amrinone infusion resulted in a reduced lactate accumulation and enhanced indocyanine green elimination, which is a reliable indicator of hepatic blood flow and of hepatocellular function. However, the clinical application of amrinone with intention to improve the ischemia

reperfusion injury was limited in experience. Further studies seem to be mandatory to confirm the potential.

In conclusion, the present results demonstrated that amrinone had pharmacological effects that contributed to the amelioration of rat ischemia–reperfusion injury. These favorable results may have been due to the modulation of intracellular cAMP levels in the liver, which might be related to augmented hepatic tissue blood flow, the inhibition of platelet aggregation and the down-regulation of ICAM-1 expression.

Acknowledgements

This work was supported by a Grant-in-aid for Scientific Research from the Ministry of Education, Culture, Sports, Science and Technology of Japan, Public Trust Fund for the Promotion of Surgery, Welfide Medical Research Foundation, Mitsui Life Social Welfare Foundation, and a Grant-in-aid for Research on Human Genome, Tissue Engineering, Food Biotechnology, Health Sciences Research Grants, Ministry of Health, Labor and Welfare of Japan.

References

[1] Benotti JR, Grossman W, Braunwald E, Davolos DD, Alousi AA. Hemodynamic assessment of amrinone. A new inotropic agent. N Engl J Med 1978;299:1373–1377.
[2] Benotti JR, Grossman W, Braunwald E, Carabello BA. Effects of amrinone on myocardial energy metabolism and hemodynamics in patients with severe congestive heart failure due to coronary artery disease. Circulation 1980;62:28–34.
[3] Likoff MJ, Weber KT, Andrews V, Janicki JS, Sutton MS, Wilson H, et al. Amrinone in the treatment of chronic cardiac failure. J Am Coll Cardiol 1984;3:1282–1290.
[4] Lanza F, Beretz A, Stierle A, Corre G, Cazenave JP. Cyclic nucleotide phosphodiesterase inhibitors prevent aggregation of human platelets by raising cyclic AMP and reducing cytoplasmic free calcium mobilization. Thromb Res 1987;45:477–484.
[5] Pattison A, Astley N, Eason CT, Bonner FW. A comparison of the effects of three positive inotropic agents (amrinone, milrinone and medorinone) on platelet aggregation in human whole blood. Thromb Res 1990;57:909–918.
[6] Mitsuoka H, Suzuki S, Sakaguchi T, Baba S, Miwa M, Konno H, et al. Contribution of endothelin-1 to microcirculatory impairment in total hepatic ischemia and reperfusion injury. Transplantation 1999;67:514–520.
[7] Sugawara Y, Kubota K, Ogura T, Esumi H, Inoue K, Takayama T, et al. Increased nitric oxide production in the liver in the perioperative period of partial hepatectomy with Pringle's maneuver. J Hepatol 1998;28:212–220.
[8] Born GVR. Aggregation of blood platelets by adenosine diphosphate and its reversal. Nature 1962;194:927–929.
[9] Sikujara O, Monden M, Toyoshima K, Okamura J, Kosaki G. Cytoprotective effect of prostaglandin I2 on ischemia-induced hepatic cell injury. Transplantation 1983;36:238–243.
[10] Chomczynski P, Sacchi N. Single-step method of RNA isolation by acid guanidinium thiocyanate–phenol–chloroform extraction. Anal Biochem 1987;162:156–159.
[11] Inoue K, Sugawara Y, Kubota K, Takayama T, Makuuchi M. Induction of type 1 plasminogen activator inhibitor in human liver ischemia and reperfusion. J Hepatol 2000;33:407–414.
[12] Hellerbrand C, Wang SC, Tsukamoto H, Brenner DA, Rippe RA. Expression of intercellular adhesion molecule 1 by activated hepatic stellate cells. Hepatology 1996;24:670–676.
[13] Liu P, Xu B, Hock CE, Nagele R, Sun FF, Wong PY. NO modulates P-selectin and ICAM-1 mRNA expression and hemodynamic alterations in hepatic I/R. Am J Physiol 1998;275:H2191–H2198.
[14] Mochida S, Ohno A, Arai M, Tamatani T, Miyasaka M, Fujiwara K. Role of adhesion molecules in the development of massive hepatic necrosis in rats. Hepatology 1996;23:320–328.
[15] Sugawara Y, Mizugaki Y, Uchida T, Torii T, Imai S, Makuuchi M, et al. Detection of Epstein–Barr virus (EBV) in hepatocellular carcinoma tissue: a novel EBV latency characterized by the absence of EBV-encoded small RNA expression. Virology 1999;256:196–202.
[16] Peterson GL. A simplification of the protein assay method of Lowry et al. which is more generally applicable. Anal Biochem 1977;83:346–356.
[17] Schierwagen C, Bylund-Fellenius AC, Lundberg C. Improved method for quantification of tissue PMN accumulation measured by myeloperoxidase activity. J Pharmacol Methods 1990;23:179–186.
[18] Suzuki S, Toledo-Pereyra LH, Rodriguez FJ, Cejalvo D. Neutrophil infiltration as an important factor in liver ischemia and reperfusion injury. Transplantation 1993;55:1265–1272.
[19] Gujral JS, Bucci TJ, Farhood A, Jaeschke H. Mechanism of cell death during warm hepatic ischemia–reperfusion in rats: apoptosis or necrosis? Hepatology 2001;33:397–405.
[20] Kohli V, Selzner M, Madden JF, Bentley RC, Clavien PA. Endothelial cell and hepatocyte deaths occur by apoptosis after ischemia–reperfusion injury in the rat liver. Transplantation 1999;67:1099–1105.
[21] Cursio R, Gugenheim J, Ricci JE, Crenesse D, Rostagno P, Maulon L, et al. A caspase inhibitor fully protects rats against lethal normothermic liver ischemia by inhibition of liver apoptosis. FASEB J 1999;13:253–261.
[22] Weishaar RE, Kobylarz-Singer DC, Steffen RP, Kaplan HR. Subclasses of cyclic AMP-specific phosphodiesterase in left ventricular muscle and their involvement in regulating myocardial contractility. Circ Res 1987;61:539–547.
[23] Ogawa S, Koga S, Kuwabara K, Brett J, Morrow B, Morris SA, et al. Hypoxia-induced increased permeability of endothelial monolayers occurs through lowering of cellular cAMP levels. Am J Physiol 1992;262:C546–C554.
[24] Tomita I, Sawa M, Munakata T, Tanaka K, Kasai S. The beneficial effect of dibutyryl cyclic adenosine monophosphate on warm ischemic injury of the rat liver induced by cardiac arrest. Transplantation 1996;62:167–173.
[25] Stelzner TJ, Weil JV, O'Brien RF. Role of cyclic adenosine monophosphate in the induction of endothelial barrier properties. J Cell Physiol 1989;139:157–166.
[26] Muller JM, Vollmar B, Menger MD. Pentoxifylline reduces venular leukocyte adherence ("reflow paradox") but not microvascular "no reflow" in hepatic ischemia/reperfusion. J Surg Res 1997;71:1–6.
[27] Lautt WW, Greenway CV. Conceptual review of the hepatic vascular bed. Hepatology 1987;7:952–963.
[28] Yadav SS, Howell DN, Steeber DA, Harland RC, Tedder TF, Clavien PA. P-selectin mediates reperfusion injury through neutrophil and platelet sequestration in the warm ischemic mouse liver. Hepatology 1999;29:1494–1502.
[29] Cywes R, Mullen JB, Stratis MA, Greig PD, Levy GA, Harvey RC, et al. Prediction of the outcome of transplantation in man by platelet adherence in donor liver allografts. Evidence of the importance of preservation injury. Transplantation 1993;56:316–323.
[30] Sill JC, Bertha B, Berger I, Uhl C, Nugent M, Folts J. Human platelet Ca^{2+} mobilization, glycoprotein IIb/IIIa activation, and experimental coronary thrombosis in vivo in dogs are all inhibited by the inotropic agent amrinone. Circulation 1997;96:1647–1653.
[31] Dustin ML, Rothlein R, Bhan AK, Dinarello CA, Springer TA. Induc-

tion by IL 1 and interferon-gamma: tissue distribution, biochemistry, and function of a natural adherence molecule (ICAM-1). J Immunol 1986;137:245–254.

[32] Yadav SS, Howell DN, Gao W, Steeber DA, Harland RC, Clavien PA. L-selectin and ICAM-1 mediate reperfusion injury and neutrophil adhesion in the warm ischemic mouse liver. Am J Physiol 1998;275:G1341–G1352.

[33] Nakano H, Kuzume M, Namatame K, Yamaguchi M, Kumada K. Efficacy of intraportal injection of anti-ICAM-1 monoclonal antibody against liver cell injury following warm ischemia in the rat. Am J Surg 1995;170:64–66.

[34] Marubayashi S, Oshiro Y, Maeda T, Fukuma K, Okada K, Hinoi T, et al. Protective effect of monoclonal antibodies to adhesion molecules on rat liver ischemia–reperfusion injury. Surgery 1997;122:45–52.

[35] Orii R, Sugawara Y, Hayashida M, Yamada Y, Chang K, Takayama T, et al. Effects of amrinone on ischaemia–reperfusion injury in cirrhotic patients undergoing hepatectomy: a comparative study with prostaglandin E1. Br J Anaesth 2000;85:389–395.

World J. Surg. 26, 105–110, 2002
DOI: 10.1007/s00268-001-0189-y

WORLD
Journal of
SURGERY

Preoperative Portal Embolization in Patients with Hepatocellular Carcinoma

Yasuhiko Sugawara, M.D.,[1,2] Junji Yamamoto, M.D.,[1] Hisato Higashi, M.D.,[1] Susumu Yamasaki, M.D.,[1] Kazuaki Shimada, M.D.,[1] Tomoo Kosuge, M.D.,[1] Tadatoshi Takayama, M.D.,[2] Masatoshi Makuuchi, M.D.[2]

[1]Department of Hepatobiliary Pancreatic Surgery, National Cancer Center Hospital, 5-1-1 Tsukiji, Chuo-ku, Tokyo 104-0045, Japan
[2]Department of Surgery, Hepatobiliary Pancreatic Surgery Division, Graduate School of Medicine, University of Tokyo, 7-3-1 Hongo, Bunkyo-ku, Tokyo 113-0033, Japan

Published Online: November 26, 2001

Abstract. The factors that contribute to the effect of portal vein embolization before hepatectomy for hepatocellular carcinoma are unclear. Sixty-six patients with hepatocellular carcinoma were enrolled in the study. Changes in liver function, portal vein pressure, and liver volume after embolization were examined. A multiple linear regression analysis was performed to identify factors that independently contributed to the effects of portal vein embolization. The acceptable volume ratio of the remnant liver was calculated from liver function and compared with the volume ratio of the non-embolized liver. No postoperative deaths were observed after portal vein embolization or hepatectomy. Serum total bilirubin and prothrombin time did not change significantly after portal vein embolization. In patients who underwent arterial embolization before portal vein embolization, aminotransferase levels increased significantly. The only factor that could significantly predict the atrophy effects of portal vein embolization was previous arterial embolization. The volume ratio of the non-embolized liver was smaller than the acceptable volume ratio of the remnant liver in 18 of 40 patients and increased over the acceptable volume ratio in all cases after portal vein embolization. Portal vein embolization induced atrophy or hypertrophy of the embolized or non-embolized liver sufficiently, even when the liver was dysfunctional or cirrhotic. The atrophy effects were significant, especially when arterial embolization had been performed before portal vein embolization.

Although recent therapeutic advances have been made in nonsurgical methods, such as percutaneous ethanol injection [1] and transarterial chemoembolization (TACE), surgical resection still remains the primary treatment for hepatocellular carcinoma (HCC) and is thought to be the only method for achieving long-term disease-free survival [2]. However, because of the high incidence of liver cirrhosis or fibrosis, and the malignant nature of the tumor, as characterized by vascular invasion or intrahepatic spread, the resectability rate for HCC has remained low, ranging from 27% to 57% [3–5]. Furthermore, over 60% of HCCs larger than 5 cm in diameter remain unresectable [4].

Since 1982, we have performed preoperative portal vein embolization (PVE) for major hepatectomy in patients with metastatic tumors, hilar cholangiocarcinoma, and HCC [6, 7]. The concept of PVE is based on the well-known phenomenon of atrophy and hypertrophy, which reflects the compensatory capacity of the structural and functional state of the liver [8, 9]. Atrophy is induced in the part of the liver that is planned to be resected by portal vein embolization and is followed by compensatory hypertrophy of the remaining part of the liver.

It would be interesting for hepatologists and liver surgeons to assess the functional and morphologic changes of the liver induced by PVE. Some papers have reported surgical results after hepatectomy following PVE. However, the underlying diseases of the patients in most of the reports were hilar cholangiocarcinoma [7, 10, 11], metastatic tumors [12, 13], and mixtures of several indications [9, 14–16]. Considering the role of PVE in hepatectomy, the liver with HCC must be analyzed separately from such cases, which are often associated with cirrhosis or treated with TACE. Moreover, the reports on PVE for HCC [17–22] have dealt with small numbers of patients (from 1 to 21). As a result, they only described the changes in some clinical factors or the surgical results of hepatectomy and failed to assess the factors that affect liver hypertrophy or the atrophy effect of PVE.

To better understand the role of PVE in liver surgery, the aim of the present study was to clarify the factors that contributed the mc ı o the effect of PVE in 66 patients who underwent hepatectomy for HCC.

Patients and Methods

Patients

At the National Cancer Center Hospital, Tokyo, 1410 hepatic resections were performed for HCC during the 15-year period from January 1984 to December 1998. Our criteria for PVE have been described previously [9]. Sixty-six patients who underwent PVE for hepatectomy in the treatment of HCC were entered in the present study. Of these, 47 patients underwent TACE prior to PVE. The interval between the latest TACE and PVE ranged from 28 to 58 days, with a median of 42 days. The 56 men and 10

Correspondence to: J. Yamamoto, M.D., Department of Hepatobiliary Pancreatic Surgery of National Cancer Center Hospital, 5-1-1, Tsukiji, Chuo-ku, Tokyo 104-8654, Japan, e-mail: jyamamot@ncc.go.jp

women ranged in age from 45 to 73 years, with a mean age of 57 years. Patient follow-up until December 1998 ranged from 3.0 to 145.3 months, with a mean of 48.2 months.

Of the 25 patients who underwent the operation before 1990, 14 were hepatitis B virus-related antigen or antibody-positive and the remaining 11 were negative (i.e., nonA and nonB hepatitis). Of the 41 patients after 1990, 14 were hepatitis C antibody-positive, 19 were hepatitis B virus-related antigen or antibody-positive, 7 were positive to both, and 1 was negative to both. Pathologically, the nontumorous area included chronic hepatitis in 50 patients and cirrhosis in 16. Conversely, the tumor tissues consisted of well-differentiated HCC in 12 cases, moderately differentiated HCC in 44, poorly differentiated HCC in 9, and HCC combined with cholangiocarcinoma in 1. The interval between PVE and hepatectomy ranged from 11 to 56 days, with a median of 21 days. Morbidity and mortality after PVE and hepatectomy were examined. Survival time was calculated from the date of liver resection until death or recurrence.

PVE Technique

PVE was carried out either via a transileocecal approach (TI-PVE, $n = 41$) or via a percutaneous transhepatic approach (PT-PVE, $n = 25$) as described previously [6, 12, 15]. TI-PVE was the preferred method and PT-PVE was conducted in patients in our early experience (before 1987) or who had undergone previous surgery of the lower abdomen resulting in severe adhesion in that area. Briefly, in TI-PVE, a 7F polyethylene catheter was inserted into the portal vein at laparotomy through the ileocolic vein. After portography had defined the intrahepatic portal anatomy, the portal venous branch of the lobe or segment to be resected was embolized under fluoroscopic control. In PT-PVE, the portal venous branch considered for embolization is punctured through ultrasound-guidance and a 6F catheter is introduced followed by portography and embolization.

The embolizing material consisted of a mixture of Gelfoam (Upjohn, Kalamazoo, MI, USA) powder, diatrizoate sodium meglumine (60% Urografin, Schering AG, Berlin, Germany, 20 to 40 ml) and gentamicin (40 mg). In nine of the patients, 5000 units of thrombin (Yoshitomi Co., Ohita, Japan) was added to the material. Immediately after embolization of all of the portal venous branches, portography was performed again to confirm the efficacy of embolization. The pressure of the portal vein trunk was measured before and after PVE in all patients. The right portal venous branch was embolized in 40 patients, the anterior branch of the right portal vein in 12, the posterior branch in 8, and the left portal venous branch in 6.

The liver can be separated into three segments based on the three branches of the Glissonean pedicle [23]: left, middle (right anterior), and right (right posterior). These three segments are about the same size and each comprises about 30% of the total volume [23]. Based on this concept of segmentation of the liver, the patients were divided into two groups according to the embolized branches: the right portal venous branch was embolized in 40 patients (Rt group) and other branches were embolized in 26 (Ot group). The average pre- and post-PVE portal vein pressures were compared in each group.

Evaluation of the Effect of Embolization

Depletion of portal blood flow to the embolized segments was evaluated repeatedly by Doppler ultrasound (Aloka, Multi-view 2000, Tokyo, Japan) until hepatectomy was accomplished. The patients were divided into two groups: those who underwent TACE before PVE (TACE+ group) and those without TACE (TACE− group). The serum transaminase levels were measured before PVE and 1, 3, 7, and 14 days after PVE, and the levels were compared with those before PVE in each group. The indocyanine green retention rate at 15 minutes (ICGR15), prothrombin time (PT), and albumin (Alb) and total bilirubin (TB) levels were also examined, and the data before and after PVE were compared.

The ratio of the volume of the non-embolized lobe to that of the whole liver before PVE and that 2 to 3 weeks after PVE were calculated using computed tomography (CT) and compared in the Rt and Ot groups. The hypertrophy and atrophy ratio were defined as follows and calculated from CT volume metric analysis in the Rt and Ot groups:

$$\text{Hypertrophy ratio (\%)} = 100 \times \text{volume of the non-embolized lobe 2–3 weeks after PVE/that before PVE}$$

$$\text{Atrophy ratio (\%)} = 100 \times \text{volume of the embolized lobe 2–3 weeks after PVE/that before PVE}$$

A multiple linear regression analysis (forward elimination method) was performed in Rt patients to identify factors that independently affected the hypertrophy and atrophy effects of PVE. The factors considered were age, gender, TACE+ or TACE−, total bilirubin, transaminase, ICGR15, TI-PVE/PT-PVE, interval between PVE and hepatectomy, pre-PVE right to left lobar volume ratio, pre-PVE portal vein pressure, and increase in portal vein pressure.

Evaluation of the Effect of Embolization

From the ICGR15 data, an acceptable volume ratio of the remnant liver was calculated according to Takasaki's equation [24]:

$$\text{Acceptable volume ratio} = 100 \times (2\text{-}\log_{10}(A))/(2\text{-}\log_{10}(\text{ICG15}))$$

(A is 40 in cirrhotic liver and 50 when noncirrotic.)

This was compared with the ratio of the volume of the non-embolized lobe to that of the whole liver before PVE and that 2 to 3 weeks after PVE in each case.

The analysis in this section was carried out using the data from Rt patients to assess a uniform PVE procedure.

Statistics

The data are expressed as means ± standard error of the mean (SEM). Survival curves were generated using the Kaplan-Meier method. Serum transaminase levels were compared with those before PVE using an analysis of variance (ANOVA) with Bonferroni's correction. Pre-PVE ICGR15, PT, Alb, TB, portal vein pressure, and liver volume ratio were compared with those post-

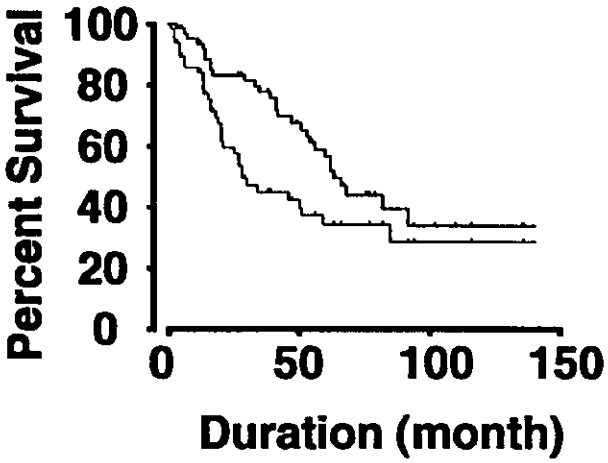

Fig. 1. Overall (top line) and disease-free (bottom line) survival rates of the patients (n = 66).

PVE by Student's t test. The hypertrophy and atrophy ratios in the groups were also compared using Student's t test. Differences were considered significant at $p < 0.005$ in ANOVA and at $p < 0.05$ in the other analyses.

Results

Surgical Results

No postoperative deaths were observed after PVE or hepatectomy. Nineteen patients had a high fever over 38°C for more than 2 days after PVE. Three patients who underwent TI-PVE suffered from mechanical ileus, which was treated conservatively.

Liver resection was performed as planned preoperatively in 61 of the 66 patients. Among Rt patients, right lobectomy was performed in 29 and extended right lobectomy was performed in 10. In 10 patients who underwent anterior branch embolization, anterior segmentectomy was performed in 7 and central bisegmentectomy (corresponding to removal of the right anterior and left medial segments according to Healey's nomenclature for liver segmentation [25]) was performed in 2. Seven of nine patients who underwent posterior branch embolization underwent posterior segmentectomy, and six of seven patients who underwent left branch embolization underwent left lobectomy. The area resected in five patients was smaller than expected. One patient in the Rt group underwent resection of an anterosuperior subsegment because a new lesion was found in the left lateral segment, which necessitated left lateral resection. In four patients in the Ot group, the operation consisted of limited resections of multiple tumors, some of which were not diagnosed preoperatively.

A single tumor was resected in 45 patients and multiple tumors (2–12) were resected in 21. The diameter of the largest tumors ranged from 1.4 cm to 19 cm, with a median of 5.5 cm. The weight of the resected specimen ranged from 270 g to 1510 g, with a median of 665 g. The morbidity rate after hepatectomy was 19.7%. Postoperative complications included pleural effusion in six, bile leakage from the dissection plane of the liver in five, and wound infection in two, which were treated conservatively.

Long-term surgical results are shown in Figure 1. The cumulative overall survival rates at 3 and 5 years were 81.2% and 58.9%,

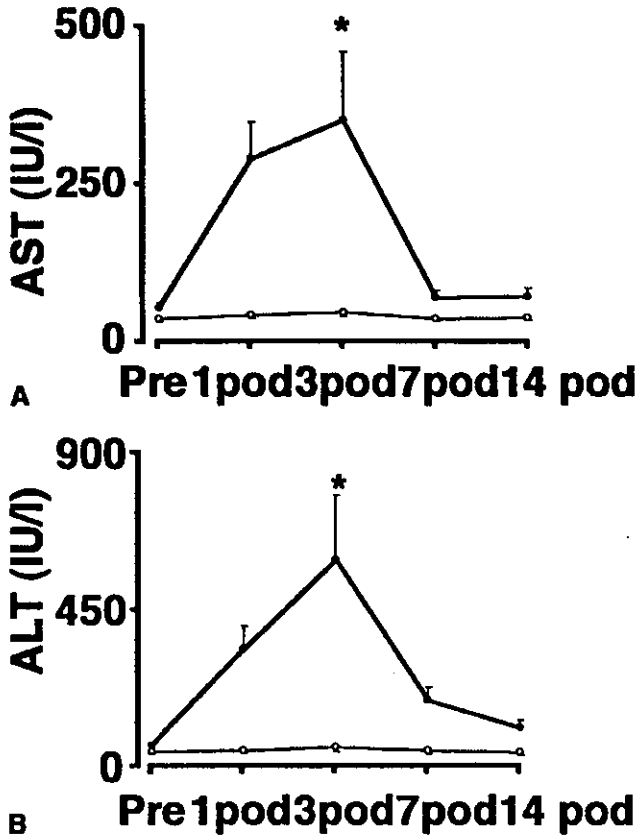

Fig. 2. Changes in the average aspartate aminotransferase (AST) (A) and alanine aminotransferase (ALT) (B) levels in the transarterial chemoembolization (TACE) positive (n = 47, thick line with closed circles) and TACE negative (n = 19, thin line with open circles) groups. *$p < 0.005$ compared with the preoperative levels in each group.

respectively, while the disease-free survival rates at 3 and 5 years were 44.1% and 37.9%, respectively. These results were compatible with our long-term results for all HCC [26].

Changes in Transaminase, ICGR15, PT, Alb, and TB Levels

In the TACE+ group, serum aspartate aminotransferase (AST) levels increased significantly 1 day after PVE compared with the preoperative levels ($p < 0.005$), and reached a maximum 3 days after PVE (Fig. 2A). In contrast, in the TACE− group, there were no significant changes during the observation period. The average alanine aminotransferase (ALT) levels showed a pattern of change similar to that of AST (Fig. 2B).

No significant difference was recognized between the pre- and post-PVE levels of ICGR15, PT, Alb, and TB (Fig. 3).

Changes in Portal Vein Pressure and Liver Volume

In the Rt group (n = 40), the portal vein pressure increased from 14.9 ± 0.8 to 22.7 ± 1.0 cmH_2O ($p < 0.0001$, Fig. 4A). In the Ot group (n = 26), it increased from 13.8 ± 1.1 to 15.6 ± 1.2 cmH_2O (p = 0.01).

The average ratio of the volume of the non-embolized lobe to that of the whole liver changed significantly from 35.5 ± 1.8% to

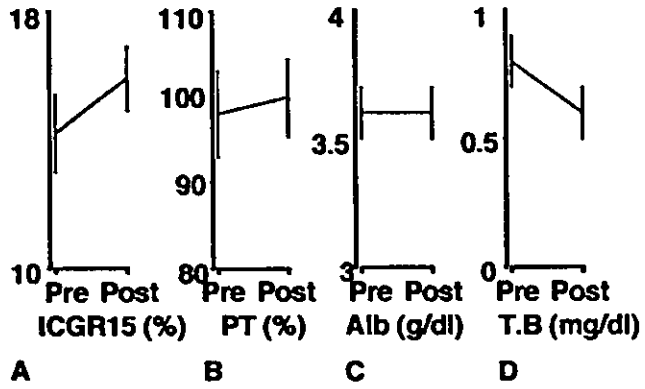

Fig. 3. Comparison of pre- and post-portal vein embolization (PVE) levels of indocyanine green retention rate at 15 minutes (ICGR15) (A), prothrombin time (PT; B), albumin (Alb; C) and total bilirubin (T.B; D). There was no significant difference in each comparison.

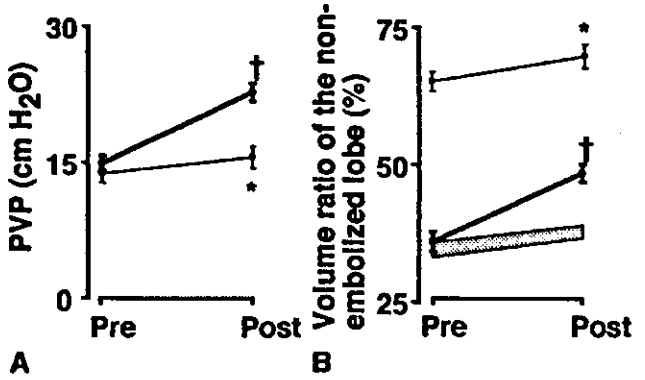

Fig. 4. Changes in pre- and post-PVE portal venous pressure (PVP) levels (A) and volume ratio of the non-embolized lobe (B) in the Rt (n = 40, thick line) and Ot (n = 26, thin line) groups. In the Rt group, the acceptable volume ratio (crosshatched zone) is shown with the volume ratio of the non-embolized lobe. $^{*}p < 0.05$ and $^{\dagger}p < 0.0001$.

48.2 ± 1.6% in the Rt group ($p < 0.0001$, Fig. 4B). In the Ot group, this ratio changed from 65.0 ± 1.8% to 69.7 ± 2.2% (p = 0.03).

The hypertrophy and atrophy ratio in the Rt group were 138.4 ± 7.8% and 82.7 ± 2.1%, respectively. In contrast, those in the Ot group were 109.7 ± 5.8% and 86.8 ± 4.1%, respectively. There was a significant difference between the groups for both values: p = 0.01 for hypertrophy and p = 0.04 for the atrophy ratio.

Multivariate Analysis

A multiple linear regression analysis revealed that only TACE+ or TACE− significantly predicted the atrophy effects of PVE (R^2 = 0.453, p = 0.0006). Other factors, including age, gender, TB, transaminase, ICGR15, TI-PVE or PT-PVE, interval between PVE and hepatectomy, pre-PVE portal vein pressure, and the increase of portal vein pressure, were not significant. None of the factors examined significantly predicted the hypertrophy effects of PVE.

The acceptable liver volume ratio of the remnant liver (n = 40) was compared with the ratio of the volume of the non-embolized lobe to that of the whole liver. Before PVE, in 18 of 40 patients, the left lobe volume ratio (35.5 ± 1.8%) was smaller than the acceptable liver volume ratio of the remnant liver (34.1 ± 1.3%). However, after PVE, the left lobe volume ratio (48.2 ± 1.6%) was larger than the acceptable ratio (37.3 ± 1.1%, Fig. 4B) in all of the patients.

Discussion

In recent reports regarding the surgical results after major hepatectomy for HCC [27–29], the mortality rates have ranged from 7% to 11%. Therefore, the low morbidity and zero mortality for hepatectomy following PVE is a noteworthy result of the present analysis and is comparable with the results in institutions with considerable experience in hepatectomy [30, 31]. PVE in selected patients with HCC could help to enhance resectability and extend the surgical indications. It is not uncommon for new lesions to be found intraoperatively [32]. When the resected volume exceeds the acceptable ratio due to resection of the new lesions, the planned liver resection area must be reduced for safety, and part of the embolized liver should be left unresected.

The significant difference in hypertrophy and atrophy effects between the groups suggested that the volume of the embolized liver could contribute to the effect of embolization. The present study also revealed that previous TACE significantly predicted the atrophy effects of PVE. In contrast, no factors significantly predicted the hypertrophy effects, although the pre-PVE right-to-left lobar volume ratio, previous TACE, and an increase in portal vein pressure had been expected to be such factors. A previous study [14] in patients with hilar cholangiocarcinoma demonstrated that total bilirubin levels before biliary drainage and a high TB level at the time of PVE accelerated the atrophy of the embolized lobe. In contrast, the future remnant liver volume before PVE significantly predicted the hypertrophy effect. These contradictory results may be due to differences in the underlying disease of the liver.

Although the factors that predicted the hypertrophy effects in our series differed from previous results [14], the hypertrophy ratios were similar among the studies (138.4 ± 7.8% vs. 137 ± 4.2%). This ratio was comparable with those in other series dealing with PVE performed before hepatectomy for HCC or hilar cholangiocarcinoma. Kinoshita and associates [22] performed 21 PVEs in association with hepatic artery embolization as a preoperative countermeasure against portal thrombi and to prevent metastasis of HCC. In one of the patients, the volume of the non-embolized area increased by 40% 40 days after PVE. In our earlier experience [7], CT volumetric studies were performed in two patients with hilar cholangiocarcinoma and revealed an increase in the relative size of the non-embolized lobe from 36% to 49% and 27% to 39%, respectively. The interval between PVE and hepatectomy was 11 and 13 days, respectively. In contrast, de Baere and colleagues [16] performed PVEs for 10 patients with metastatic tumors. The hypertrophy ratio was reported to be 164% 4 to 5 weeks after PVE. The lower rate of hypertrophy in our series may be due to the longer interval between PVE and hepatectomy. Other possible explanations include the presence of an underlying liver disease and low regenerative capacity of the dysfunctional liver.

Serum transaminase was significantly elevated after PVE in the TACE+ patients. The functional burden placed on the liver by

PVE was originally thought to be negligible and transient [14], as shown in the changes in the TACE− patients. However, the present finding indicated that PVE provoked substantial hepatocyte necrosis when the arterial flow of the liver was insufficient because of TACE. The hypothesized mechanism might partially explain the marked atrophic change in the embolized part of the liver in the TACE+ patients.

In summary, the present results support the notion that PVE is suitable as a pre-treatment for functionally comprised liver before extensive resection. PVE induced atrophy of the embolized liver and hypertrophy of the non-embolized liver, especially when the liver had been treated with TACE before PVE. PVE might contribute to favorable short-term results of hepatectomy in selected patients with HCC.

Résumé. Les facteurs qui contribuent aux effets de l'embolisation de la veine porte avant résection hépatique pour cancer hépatocellulaire ne sont pas clairs. Soixante-six patients ayant un cancer hépatocellulaire sont entrés dans l'étude. On a enregistré les modifications de la fonction hépatique, de la pression dans la veine porte et le volume hépatique après embolisation. Par analyse de régression linéaire multiple on a identifié les facteurs indépendants des effets de l'embolisation porte. Le rapport entre le volume du foie restant acceptable comparé au volume du foie non embolisé a été calculé à partir des tests de fonction hépatique. La mortalité après embolisation porte ou après résection hépatique a été nulle. On n'a noté aucun changement significatif dans le taux de bilirubine totale ou du temps de prothrombine après l'embolisation porte. Chez les patients qui ont eu une embolisation artérielle avant l'embolisation de la veine porte, on a remarqué une augmentation significative des transaminases. Le seul facteur prédictif des effets d'atrophie après embolisation porte a été l'embolisation artérielle antérieure. Le rapport entre le volume du foie non-embolisé et le volume du foie restant était inférieur à l'unité chez 18 des 40 patients, et il a augmenté pour dépasser l'unité après embolisation porte dans tous les cas. L'embolisation porte a induit, respectivement, l'atrophie et l'hypertrophie du foie embolisé ou non-embolisé de façon suffisante, même quand la fonction hépatique était perturbée ou quand le foie était cirrhotique. Les effets d'atrophie ont été plus importants surtout lorsque l'embolisation artérielle a été réalisée avant l'embolisation porte.

Resumen. Los efectos de la embolización de la vena porta, realizada antes de proceder a una hepatectomía como tratamiento de un carcinoma hepatocelular, no son bien conocidos. Este estudio consta de 66 pacientes aquejados de carcinoma hepatocelular. Se estudiaron los cambios tanto de la función como del volumen hepático y de la presión portal tras la embolización. Se realizó un análisis de regresión lineal múltiple para identificar los parámetros independientes que pudieran contribuir a las acciones de la embolización portal. El porcentaje del volumen del remanente hepático se calculó a partir de la función hepática y se comparó con el coeficiente volumétrico del hígado no-embolizado. Tras la embolización de la vena porta y la hepatectomía no registramos mortalidad postoperatoria alguna. Tras la embolización portal, tanto la bilirrubina sérica total como la tasa de protrombina no sufrieron modificación significativa alguna. En aquellos pacientes que fueron sometidos a una embolización arterial previa a la embolización de la vena porta, se constató un incremento significativo de los niveles de aminotransferasa. El único factor pronóstico que permite predecir la atrofia hepática tras embolización portal es la embolización arterial previa. En 18 de 40 pacientes el coeficiente volumétrico del hígado no embolizado fue menor que el aceptable coeficiente volumétrico del remanente hepático, aumentando a un porcentaje aceptable del volumen hepático en todos los casos de embolización de la vena porta. La embolización portal produce una atrofia o hipertrofia del hígado embolizado o no-embolizado, que es funcionalmente más que suficiente, incluso en hígados cirróticos o con disfunción hepática. La atrofia hepática sólo fue significativa cuando se procede a una embolización arterial previa a la embolización de la vena porta.

Acknowledgments

This study is supported in part by a Grant-in-Aid for the Comprehensive 10-Year Strategy of Cancer Control from the Ministry of Health and Welfare of Japan.

References

1. Livraghi T, Giorgio A, Marin G, Salmi A, de Sio I, Bolondi L, Pompili M, Brunello F, Lazzaroni S, Torzilli G: Hepatocellular carcinoma and cirrhosis in 746 patients: long-term results of percutaneous ethanol injection. Radiology 1995;197:101
2. Makuuchi M, Takayama T, Kubota K, Kimura W, Midorikawa, Y, Miyagawa S, Kawasaki S: Hepatic resection for hepatocellular carcinoma-Japanese experience. Hepatogastroenterology 1998;45 Suppl 3:1267
3. Farmer DG, Rosove MH, Shaked A, Busuttil RW: Current treatment modalities for hepatocellular carcinoma. Ann. Surg. 1994;219: 236
4. Kinami Y, Takashima S, Miyazaki I: Hepatic resection for hepatocellular carcinoma associated with liver cirrhosis. World J. Surg. 1986; 10:294
5. The Liver Cancer Study Group of Japan Primary liver cancer in Japan. Cancer 1984;54:1747
6. Makuuchi M, Takayasu K, Takuma T, Yamazaki S, Hasegawa H, Nishiura S, Shimamura Y: Preoperative transcatheter embolization of the portal venous branch for patients receiving extended lobectomy due to the bile duct carcinoma. J. Jpn. Soc. Clin. Surg. 1984;45:1558 (in Japanese with an English abstract)
7. Makuuchi M, Thai BL, Takayasu K, Takayama T, Kosuge T, Gunven P, Yamazaki S, Hasegawa H, Ozaki H: Preoperative portal embolization to increase safety of major hepatectomy for hilar bile duct carcinoma: a preliminary report. Surgery 1990;107:521
8. Schalm L, Bax HR, Mansen BJ: Atrophy of the liver after occlusion of the bile duct or portal vein and compensatory hypertrophy of the unoccluded portion and its clinical importance. Gastroenterology 1956;32:132
9. Makuuchi M, Kosuge T, Lygidakis NJ: New possibilities for major liver surgery in patients with Klatskin tumors or primary hepatocellular carcinoma—an old problem revisited. Hepatogastroenterology 1991;38:329
10. Nagino M, Nimura Y, Kamiya J, Kondo S, Uesaka K, Kin Y, Hayakawa N, Yamamoto H: Changes in hepatic lobe volume in biliary tract cancer patients after right portal vein embolization. Hepatology 1995;21:434
11. Kawasaki S, Makuuchi M, Miyagawa S, Kakazu T: Radical operation after portal embolization for tumor of hilar bile duct. J. Am. Coll. Surg. 1994;178:480
12. de Baere T, Roche A, Elias D, Lasser P, Lagrange C, Bousson V: Preoperative portal vein embolization for extension of hepatectomy indications. Hepatology 1996;24:1386
13. Kawasaki S, Makuuchi M, Kakazu T, Miyagawa S, Takayama T, Kosuge T, Sugihara K, Moriya Y: Resection for multiple metastatic liver tumors after portal embolization. Surgery 1994;115:674
14. Imamura H, Shimada R, Kubota M, Matsuyama Y, Nakayama A, Miyagawa S, Makuuchi M, Kawasaki S: Preoperative portal vein embolization: an audit of 84 patients. Hepatology 1999;29:1099
15. Harada H, Imamura H, Miyagawa S, Kawasaki S: Fate of the human liver after hemihepatic portal vein embolization: cell kinetic and morphometric study. Hepatology 1997;26:1162
16. de Baere T, Roche A, Vavasseur D, Therasse E, Indushekar S, Elias D, Bognel C: Portal vein embolization: utility for inducing left hepatic lobe hypertrophy before surgery. Radiology 1993;188:73
17. Wakabayashi H, Okada S, Maeba T, Maeta H: Effect of preoperative portal vein embolization on major hepatectomy for advanced-stage hepatocellular carcinomas in injured livers: a preliminary report. Surg. Today 1997;27:403
18. Shimamura T, Nakajima Y, Une Y, Namieno T, Ogasawara K, Yamashita K, Haneda T, Nakanishi K, Kimura J, Matsushita M, Sato N, Uchino J: Efficacy and safety of preoperative percutaneous

transhepatic portal embolization with absolute ethanol: a clinical study. Surgery 1997;121:135
19. Azoulay D, Raccuia JS, Castaing D, Bismuth H: Right portal vein embolization in preparation for major hepatic resection. J. Am. Coll. Surg. 1995;181:266
20. Lee KC, Kinoshita H, Hirohashi K, Kubo S, Iwasa R: Extension of surgical indications for hepatocellular carcinoma by portal vein embolization. World J. Surg. 1993;17:109
21. Nakao N, Miura K, Takahashi H, Ohnishi M, Miura T, Okamoto E, Ishikawa Y: Hepatocellular carcinoma: combined hepatic, arterial, and portal venous embolization. Radiology 1986;161:303
22. Kinoshita H, Sakai K, Hirohashi K, Igawa S, Yamasaki O, Kubo S: Preoperative portal vein embolization for hepatocellular carcinoma. World J. Surg. 1986;10:803
23. Takasaki K: Glissonean pedicle transection method for hepatic resection: a new concept of liver segmentation. J. Hepatobiliary Pancreat. Surg. 1998;5:286
24. Takasaki K: Selection of operative procedure for primary hepatocellular carcinoma, complicated with liver cirrhosis. Jpn. J. Gastroenterol. Surg. 1986;19:1881 (in Japanese)
25. Healey JEJ, Schroy PC: Anatomy of the biliary ducts within the human liver: analysis of the prevailing pattern of branching and the major variations of the biliary ducts. Arch. Surg. 1953;66:599
26. Kosuge T, Makuuchi M, Takayama T, Yamamoto J, Shimada K, Yamasaki S: Long-term results after resection of hepatocellular carcinoma: experience of 480 cases. Hepatogastroenterology 1993;40: 328
27. Farges O, Malassagne B, Flejou JF, Balzan S, Sauvanet A, Belghiti J: Risk of major liver resection in patients with underlying chronic liver disease: a reappraisal. Ann. Surg. 1999;229:210
28. Shirabe K, Shimada M, Gion T, Hasegawa H, Takenaka K, Utsunomiya T, Sugimachi K: Postoperative liver failure after major hepatic resection for hepatocellular carcinoma in the modern era with special reference to remnant liver volume. J. Am. Coll. Surg. 1999; 188:304
29. Shimada M, Gion T, Hamatsu T, Yamashita Y, Hasegawa H, Utsunomiya T, Takenaka K, Sugimachi K: Evaluation of major hepatic resection for small hepatocellular carcinoma. Hepatogastroenterology 1999;46:401
30. Fan ST, Lo CM, Liu CL, Lam CM, Yuen WK, Yeung C, Wong J: Hepatectomy for hepatocellular carcinoma: toward zero hospital deaths. Ann. Surg. 1999;229:322
31. Torzilli G, Makuuchi M, Inoue K, Takayama T, Sakamoto Y, Sugawara Y, Kubota K, Zucchi A: No-mortality liver resection for hepatocellular carcinoma in cirrhotic and non-cirrhotic patients: is there a way? A prospective analysis of our approach. Arch. Surg. 1999;134:984
32. Makuuchi M, Hasegawa H, Yamazaki S: Ultrasonically guided subsegmentectomy. Surg. Gynecol. Obstet. 1985;161:346

ELSEVIER

Journal of Hepatology 36 (2002) 210–217

Journal of Hepatology

www.elsevier.com/locate/jhep

Early induction of nerve growth factor-induced genes after liver resection–reperfusion injury

Takao Ohkubo[1,2], Yasuhiko Sugawara[1,*], Kazuki Sasaki[2], Kouji Maruyama[2], Naganari Ohkura[2], Masatoshi Makuuchi[1]

[1]*Hepatobiliary Pancreatic Surgery Division, Department of Surgery, Graduate School of medicine, University of Tokyo, 7-3-1 Hongo, Bunkyo-ku, Tokyo 113-0033, Japan*

[2]*Growth Factor Division, National Cancer Center Research Institute, 5-1-1 Tsukiji, Chuo-ku, Tokyo 104-0045, Japan*

***Background/Aims*: Nur-related factor 1 (Nurr1) has been implicated in liver generation after hepatectomy. We hypothesized that the genes in the nerve growth factor-induced gene B (NGFI-B) family was induced in liver ischemia-reperfusion injury.**

***Methods*: Expression of the NGFI-B family genes was examined by the reverse transcription-polymerase chain reaction in rat and human livers. In situ hybridization was performed to check the localization of the NGFI-B gene in rat liver. Expression of phospho-Ser-133-specific cyclic adenosine-3′:5′-monophosphate response element binding (pCREB) protein was examined by Western blot analysis and gel shift assay, since the promoter region of the NGFI-B family genes contains CRE.**

***Results*: The expression of the NGFI-B family genes were recognized within 30 min after ischemia-reperfusion in rat liver, which was augmented by cycloheximide injection. In human specimens, the NGFI-B family genes expression was stronger than that before ischemic insult. pCREB protein was detected in the rat liver sampled 15 min after reperfusion. Gel shift assay suggested that CREB bound to neuron-derived orphan receptor gene in rat liver cells.**

***Conclusions*: We recognized the early induction of the NGFI-B family genes after ischemia-reperfusion injury in rat and human livers. A pathway via CREB may be responsible for the induction.**

***Keywords*: Neuron-derived orphan receptor; Cyclic adenosine-3′:5′-monophosphate response element; Ischemia-reperfusion injury**

1. Introduction

Lipophilic hormones, including steroids, retinoids, thyroid hormones and vitamin D, have extensive physiological roles. They penetrate the membrane of target cells and exert their potent regulatory effects by binding to specific receptors [1]. These receptors are ligand-activated transcription factors that regulate the expression of target genes by binding to specific *cis*-acting sequences, known as hormone response elements, in their promoter region. Sequence and functional analyses have revealed that these receptors share a modular structure and form a large gene family called the nuclear receptor subfamily [2].

Although several members of the family have been identified [3], some of their specific ligands are not yet known. These members are called 'orphan' receptors. Nerve growth factor-induced gene B (NGFI-B), Nur-related factor 1 (Nurr1) and neuron-derived orphan receptor (NOR-1) belong to the orphan subclass of the nuclear receptor subfamily. They constitute the NGFI-B subfamily due to a common structure characterized by a central DNA-binding domain, a ligand-binding domain in the carboxyl terminus and a variable amino-terminal region.

NGFI-B was identified as a gene induced by nerve growth factor in the rat pheochromocytoma cell line PC12 [4]. Nurr1 was isolated from a neonatal mouse brain complementary DNA (cDNA) library [5]. NOR-1 was identified

Received 18 July 2001; received in revised form 30 August 2001; accepted 2 October 2001

* Corresponding author. Tel.: +81-3-3815-5411; fax: +81-3-5684-3989.
E-mail address: yasusuga-tky@umin.ac.jp (Y. Sugawara).

0168-8278/02/$20.00
PII: S0168-8278(01)00258-6

from cultured rat fetal forebrain cells [6]. These molecules have been thought to be neuron-specific factors [4–6]. Several studies have focused on the role of the NGFI-B subfamily in the nervous system [7,8]. NGFI-B-induced differentiation of rat neuronal cells is accompanied by NGFI-B expression [4]. Treatment of cultured fetal rat brain cells with antisense oligonucleotides to NOR-1 mRNA induces cell migration, extension of neurite-like processes and cell aggregation [9]. Nurr1-deficient mice have been shown to exhibit abnormal development of midbrain dopaminergic neurons and die soon after birth [10]. These findings indicate that the NGFI-B subfamily is involved in neuronal differentiation in the developing nervous system.

Scearce et al. suggested that Nurr1 is rapidly induced following partial hepatectomy in rats [11]. In their study, rats were injected with 50 mg/kg of cycloheximide and subjected to approximately 70% hepatectomy. The remaining liver was sampled at 0.5, 1, 3, 4, 6, 8, 16 and 24 h after the operation and the level of messenger RNA for Nurr1 was checked by Northern blot analysis. Nurr1 RNA was recognized in samples taken at 0.5, 1 and 3 h after the operation. Based on these results, they concluded that Nurr1 was induced during liver regeneration and called Nurr1 regenerating liver nuclear receptor (RNR-1).

This experiment raises some questions. For example, it remains unclear if Nurr1 is truly induced in the regenerating liver. DNA synthesis in the parenchymal cells starts 12–16 h after a two-thirds hepatectomy, and reaches a peak around 24 h after the operation [12]. It is possible that Nurr1 is merely induced in the liver after ischemia-reperfusion injury. The aim of this study was to explore our hypothesis in rat and human livers.

2. Materials and methods

2.1. Animals

Male Sprague–Dawley rats, weighing 275–300 g, were purchased from Nippon Bio-Supplement Center (Tokyo, Japan). The rats were fed a diet of commercial pellets and water ad libitum. They were housed in a temperature-controlled room (22 ± 2°C) under normal lighting conditions and cared for in accordance with the guidelines for animal experimentation promulgated by the Animal Research Committee, Faculty of Medicine, University of Tokyo.

2.2. Surgical procedure

Rats were fasted with free access to water for 12 h prior to the surgical procedure. Under anesthesia with ether inhalation, they were placed in a supine position and laparotomized with a midline incision. The rats were injected with 100 μg/kg of heparin.

The rats were divided into two groups: a cycloheximide group and a control. The rats in the cycloheximide group were treated with 50 mg/kg cycloheximide (Calbiochem, La Jolla, CA, USA; 5% solution in phosphate-buffered saline) 30 min before laparotomy. In the controls, the same volume of normal saline was given intraperitoneally. After laparotomy, the left branches of both the portal vein and hepatic artery were clamped with a micro-vascular clip (Bear clamp, Kyowa Precision Instruments Co., Tokyo, Japan) for 60 min to establish liver ischemia while preventing portal congestion. The clip was then released to induce reperfusion.

As a control, a sham operation was also performed on animals in each group ($n = 3$).

2.3. Blood and liver sampling

Part of the left lateral lobe was sampled at 0, 15, 30, 60 and 120 min after reperfusion ($n = 3$ for each time and each group). All of the rats in the cycloheximide group died 120 min after reperfusion, and were then omitted from the analysis. The tissue samples were frozen immediately and stored at −80°C in polystyrene tubes until use.

Blood sampling was performed from the aorta with the same time schedule, and aspartate aminotransferase (AST) levels were measured by Karmen's ultraviolet absorption test.

2.4. Reverse transcription-polymerase chain reaction (RT-PCR) and nucleotide sequencing

Transcripts of NGFI-B, NOR-1 and Nurr1 were detected by the RT-PCR, using the oligo-nucleotide primers described previously [8]. These were designed to amplify the sequences in the putative ligand-binding domains. The expected PCR products of NGFI-B, NOR-1 and Nurr1 were 358, 418 and 352 base pairs long, respectively.

Total RNA was isolated by guanidine thiocyanate extraction [13] and 5 μg of RNA was used for complementary DNA synthesis with a specific downstream antisense primer and a First Strand cDNA Synthesis kit (Pharmacia LKB Biotechnology Inc., Piscataway, NJ, USA), according to the manufacturer's protocol.

PCR was performed using a Thermal Cycler 480 (Perkin–Elmer, Foster City, CA, USA) at the following temperatures: for NGFI-B (28 cycles), denaturation at 95°C for 1 min, primary annealing at 74°C for 2 min and primer extension at 72°C for 3 min; for NOR-1 (30 cycles), 95°C for 1 min, 68°C for 2 min and 72°C for 3 min and for Nurr1 (32 cycles), 95°C for 1 min, 66°C for 2 min and 72°C for 3 min. Under these conditions, the amount of PCR product was almost proportional to the amount of the cDNA template [8]. The PCR products were run on a 2.5% agarose gel and visualized by ethidium bromide staining.

2.5. Quantitative mRNA analysis of NGFI-B family genes

The amounts of NGFI-B, NOR-1 and Nurr1 mRNA were measured by quantitative RT-PCR using an internal standard RNA as described previously [14]. Briefly, the cDNA of mRNA of each gene was generated in a single tube by reverse transcription of total RNA (5 μg) in the presence of 0.05, 0.5 and 0.05 amol of internal standard RNA of each gene, along with a mixture of the corresponding specific antisense primers.

The cDNA of each mRNA was amplified separately by PCR with a specific primer, where the sense primer was labeled with fluorescein isothiocyanate (FITC). PCR consisted of 40 cycles of 1 min at 95°C, 2 min at 66°C and 3 min at 72°C, with a final extension at 72°C for 10 min. The amount of fluorescent PCR product was measured using a capillary DNA sequencer (ABI PRISM 310, Perkin–Elmer).

The amount of mRNA of each gene was determined by multiplying the amount of the internal standard RNA by the ratio of the authentic product of each gene to that derived from the corresponding internal standard RNA.

2.6. Southern blot analysis of the PCR product

The agarose gel was transferred to a nylon membrane (Hybond N, Amersham, Buckinghamshire, UK). Hybridization with ^{32}P-labeled NGFI-B, NOR-1 and Nurr1 cDNA of the entire coding region was performed overnight at 42°C. The membrane was washed three times in saline sodium citrate and 0.1% sodium dodecyl sulfate (SDS) at 50°C, and auto-radiographed.